Article

Predator mass mortality events restructure food webs through trophic decoupling

Simon P. Tye[1✉], Samuel B. Fey[2], Jean P. Gibert[3] & Adam M. Siepielski[1✉]

Predators have a key role in structuring ecosystems[1–4]. However, predator loss is accelerating globally[4–6], and predator mass-mortality events[7] (MMEs)—rapid large-scale die-offs—are now emblematic of the Anthropocene epoch[6]. Owing to their rare and unpredictable nature[7], we lack an understanding of how MMEs immediately impact ecosystems. Past predator-removal studies[2,3] may be insufficient to understand the ecological consequences of MMEs because, in nature, dead predators decompose in situ and generate a resource pulse[8], which could alter ensuing ecosystem dynamics by temporarily enhancing productivity. Here we experimentally induce MMEs in tritrophic, freshwater lake food webs and report ecological dynamics that are distinct from predator losses[2,3] or resource pulses[9] alone, but that can be predicted from theory[8]. MMEs led to the proliferation of diverse consumer and producer communities resulting from weakened top-down predator control[1–3] and stronger bottom-up effects through predator decomposition[8]. In contrast to predator removals alone, enhanced primary production after MMEs dampened the consumer community response. As a consequence, MMEs generated biomass dynamics that were most similar to those of undisturbed systems, indicating that they may be cryptic disturbances in nature. These biomass dynamics led to trophic decoupling, whereby the indirect beneficial effects of predators on primary producers are lost and later materialize as direct bottom-up effects that stimulate primary production amid intensified herbivory. These results reveal ecological signatures of MMEs and demonstrate the feasibility of forecasting novel ecological dynamics arising with intensifying global change.

MMEs are rapid, large-scale die-offs in wild animal populations[7]. In contrast to other episodic die-offs such as anadromous fish spawns or cicada emergence, MMEs simultaneously affect all life stages[7] and often decimate populations[10]. Over the past century, MMEs have increased in frequency and magnitude across most animal groups, including many predator populations[7]. The magnitudes of MMEs can be staggering—eradicating more than a billion fish, eliminating hundreds of thousands of mammals and birds, and producing hundreds of millions of tons of dead biomass almost instantly[7]. Over long timescales, these events can contribute to trophic downgrading[4] and sustained defaunation[6]. Despite progress in detecting[7] and predicting[8,11] their occurrence, our empirical understanding of their ecological repercussions is far less established. This lack of understanding precludes accurately forecasting food web responses to these increasingly frequent catastrophes.

Ecological theory on the immediate food-web consequences of predator MMEs[8] proposes that the ensuing dynamics may be explained either by the additive effects of predator losses and resource pulses[1–3], or through emergent non-additive effects of these perturbations[12,13]. These predictions remain untested and hinge on two key features of MMEs[8]: (1) rapidly weakened top-down (that is, predator controlled) effects, which release intermediate trophic levels from predation but increase consumption at lower trophic levels[1–3,14]; and (2) concurrent strengthening of bottom-up (that is, resource controlled) effects as predators decompose and release nutrients[8]. These features are reminiscent of predator removals[14] and intensified resource additions[15] (for example, eutrophication)—two overarching perturbations of the Anthropocene that shaped foundational ecological theory on community structure, food-web dynamics and biomass stability[1–4,14]. Although a consensus exists about the independent effects of predator removals and resource additions on community dynamics[1–3], an expanding list of global drivers has intensified predator declines[6] and excessive nutrient additions that enhance productivity[16] since these ideas were formulated in the mid-twentieth century. Such widespread degradation raises questions about whether food web responses to predator MMEs can be adequately predicted by paradigms established in a less volatile world.

Here we used freshwater lake mesocosms to experimentally resolve the ecological aftermath of predator MMEs and determine whether foundational ecological theory can readily anticipate the structure and dynamics of post-perturbation communities. We used a freshwater lake system because it has extremely well-understood trophic links[12,13,17–20] and exhibits rapid nutrient cycling and remineralization when predators decompose[12,13] and release growth limiting nutrients[21]. Moreover, most documented MMEs have affected freshwater lake fish[7], and these

[1]Department of Biological Sciences, University of Arkansas, Fayetteville, AR, USA. [2]Department of Biology, Reed College, Portland, OR, USA. [3]Department of Biology, Duke University, Durham, NC, USA. ✉e-mail: simontye@uark.edu; amsiepie@uark.edu
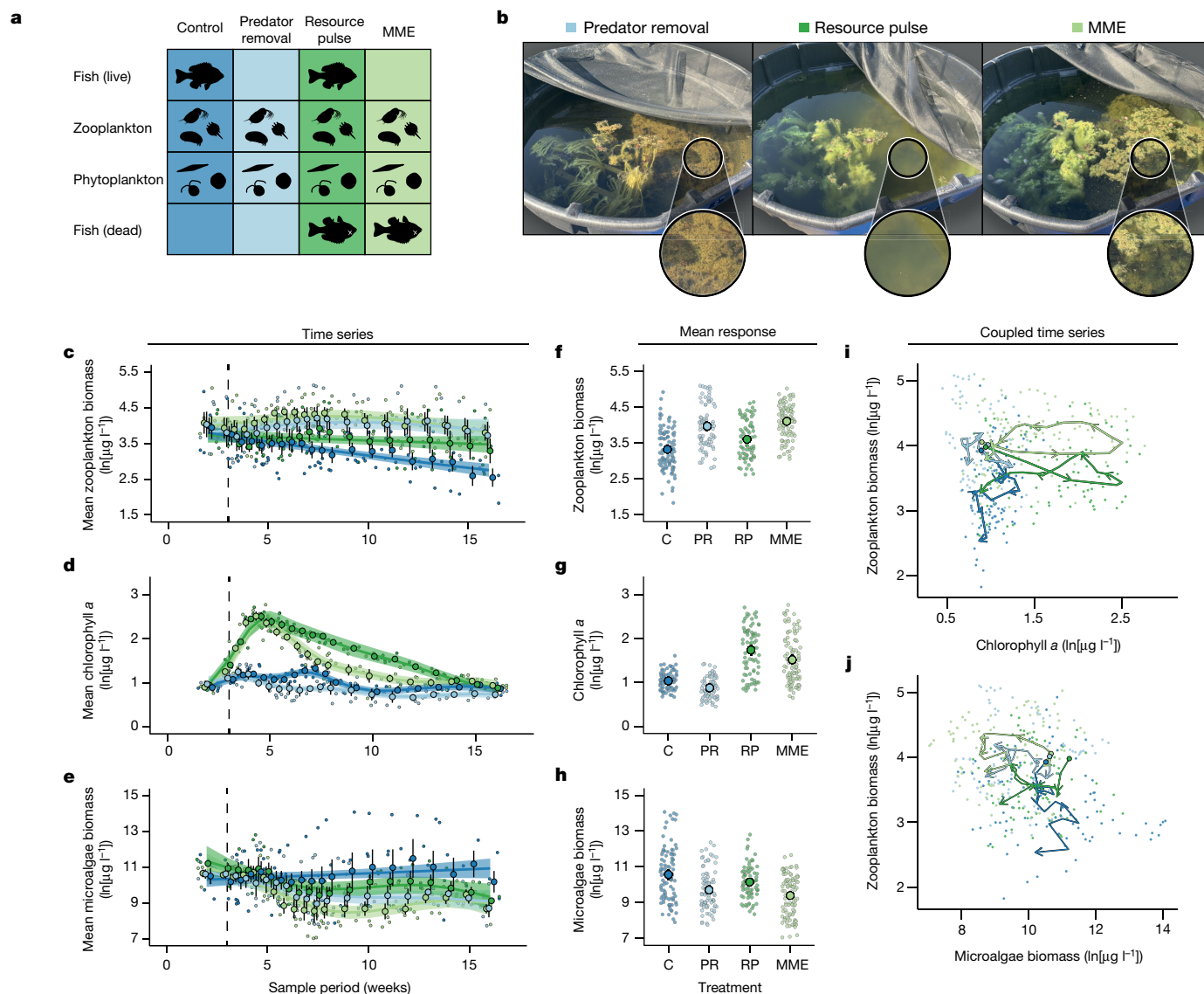
Fig. 1 | Food-web biomass responses to predator removals, resource pulses and MMEs. a, Factorial experimental design to create four ecological scenarios in tritrophic freshwater food webs: control (live fish; dark blue; $n = 5$ replicates), predator removal (no fish; light blue; $n = 4$ replicates), resource pulse (live fish with additional dead fish added; dark green; $n = 4$ replicates) and MME (dead fish; light green; $n = 5$ replicates) scenarios. **b**, A visual comparison shows illustrative photographs of each disturbance treatment. **c**–**e**, Time-series analysis of the mean consumer biomass (zooplankton; **c**) and the total production (chlorophyll a; **d**) or microalgal biomass (**e**) after inducing treatments (dashed lines) over 120 days. The solid lines and shaded regions indicate the model predictions and the 95% confidence intervals (CIs), respectively, based on smoothed moving averages (Methods). The points and lines indicate mean ± 1 s.e.m. by sampling period and treatment; points are jittered. **f**–**h**, The mean consumer biomass (**f**), total production (**g**) and microalgal biomass (**h**) responses across mesocosms and samples. The large points, lines and small points indicate the mean values, 95% CIs and raw data, respectively. **i,j**, Coupled time-series plots showing the mean consumer biomass alongside the mean producer (**i**) or microalgal biomass (**j**). The circles and arrows indicate the starting locations and direction through time, respectively. Data were analysed from 355 biologically independent samples (that is, trophic biomass estimates) for the control ($n = 96$), predator removal ($n = 80$), resource pulse ($n = 80$) and MME ($n = 96$) conditions, respectively, from one experiment. Statistical analysis was performed using a general additive mixed model (GAMM; **c**–**e**) and two-sided two-way ANOVA (**f**–**h**).

events are predicted to occur more frequently in coming decades[11]. Within mesocosms, we established simplified food webs containing phytoplankton, zooplankton and planktivorous fish, which capture the major trophic levels and links between primary producers and the top consumer in the littoral zone of lake food webs. We then implemented a 2 × 2 factorial experiment with treatments that included the presence/absence of live predators and/or predator carrion (Fig. 1a). This created an experimental control (fish present, carrion absent) and three perturbations: predator removal (fish and carrion absent), resource pulse (fish and carrion present) and MME (fish absent, carrion present). To acquire dead fish, we performed euthanasia on haphazardly selected

bluegill using a method approved by the University of Arkansas Institute of Animal Care and Use (IACUC, 191060; Methods).

To compare perturbations, we sampled large-bodied zooplankton consumers, microalgae (primary producers) and total primary production (chlorophyll a, total primary production minus herbivory; for example, the amount of standing phytoplankton biomass) for 120 days (Methods). We focused on these consumers and producers because they often exhibit strong responses to predation[22,23] and herbivory[17–19], respectively. Although our sampling methods probably missed rare species, which precludes us from drawing inferences about individual species responses, they do enable determining general ecological
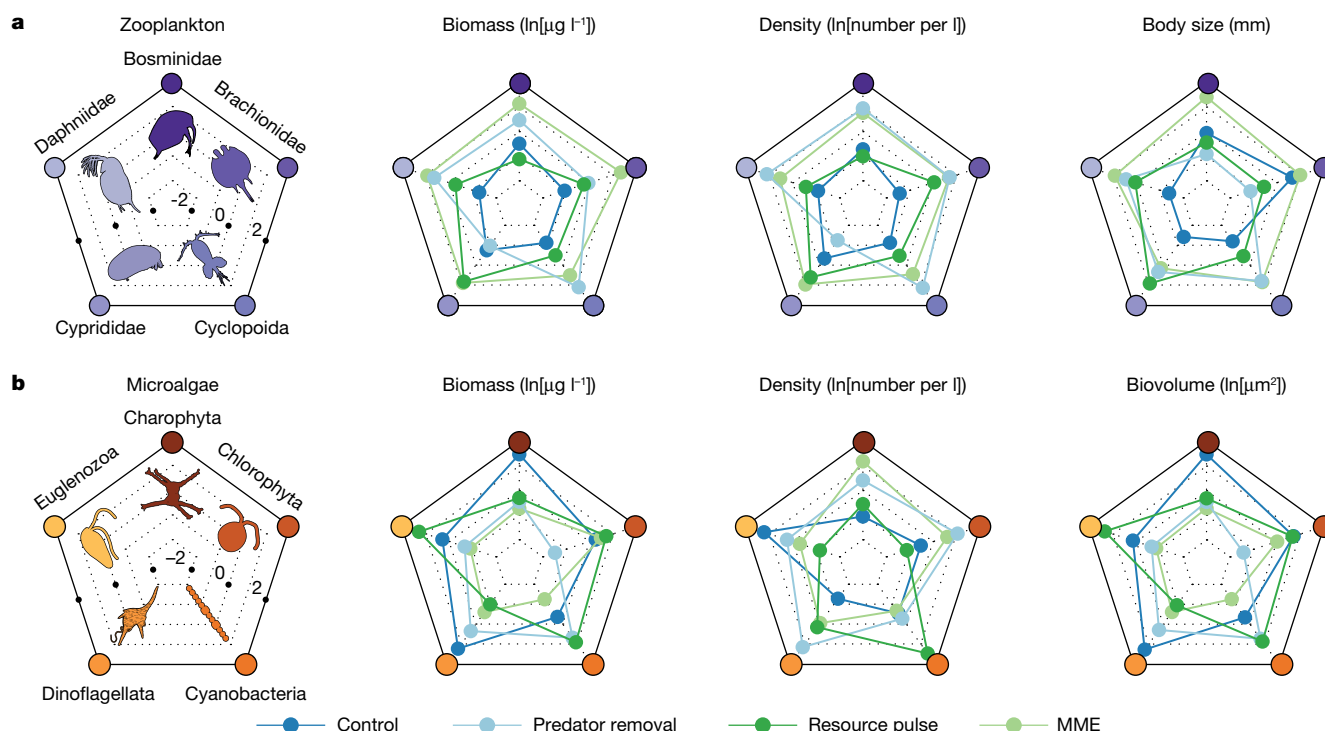
Fig. 2 | Community-wide biomass, density and functional trait responses to predator removals, resource pulses and MMEs. a,b, Community structure of consumers (zooplankton; **a**) and key producers (microalgae; **b**) in the control, predator removal, resource pulse and MME scenarios. Radar plots for zooplankton (**a**) and microalgal (**b**) biomass (ln[μg l⁻¹]), density (ln[number per l]) and key functional traits—individual body size (mm) or biovolume (ln[μm²])— by treatment. The coloured points that are connected by lines within the radar plots represent scaled and centred mean values by treatment for dominant zooplankton and microalgae. The coloured circles bordering the radar plots represent major zooplankton families (**a**) and microalgal phyla (**b**).

dynamics of trophic levels and key functional groups (family for zooplankton, phyla for microalgae) to each experimental perturbation (Methods). We first determined whether trophic biomass responses to predator MMEs can be predicted from classic theory by analysing the additive effects of predator removals (that is, fish removed) and resource pulses (that is, carrion added). In the presence of non-additive (interactive) effects, classic theory would not correctly forecast trophic biomass responses to predator MMEs. We next compared four key aspects of food webs after perturbations: community structure, ecological functional traits that influence consumer-resource interactions (that is, body size), patterns of community dynamics and the temporal stability of community biomass.

Trophic biomass responses

Our results demonstrate that predator MMEs, predator removals and resource pulses generate predictable trophic biomass responses over time, while also exhibiting distinct food web structures and dynamics (Fig. 1b–j). Relative to the control conditions, MMEs increased zooplankton biomass (general additive mixed model, +106%, $t_{9.53} = 10.78$, $P < 0.01$; Fig. 1c,f), increased total primary production (+137%, chlorophyll a, $t_{33.21} = 16.73$, $P < 0.01$; Fig. 1d,g) and decreased biomass of microalgae (−82%, $t_{13.59} = -7.80$, $P < 0.01$; Fig. 1e,h). Comparatively, predator removals strongly increased the zooplankton biomass (+95%, $t_{9.53} = 8.64$, $P < 0.01$; Fig. 1c,f), but decreased the total primary production (−22%, $t_{33.21} = -7.57$, $P < 0.01$; Fig. 1d,g) and decreased the microalgal biomass (−75%, $t_{13.59} = -5.26$, $P < 0.01$; Fig. 1e,h), whereas resource pulses primarily increased the total production (+195%, $t_{33.21} = 22.54$, $P < 0.01$; Fig. 1d,g). Distinct trophic biomass responses to perturbations were particularly evident when comparing coupled time series (Fig. 1i,j). Only MMEs led to concurrent proliferation of consumers and producers (Fig. 1i), yet overall declines in microalgae (Fig. 1j), which highlighted

the capacity for zooplankton herbivory to rapidly regulate these resources[17–19].

While previous research has indicated that excessive resource inputs can strengthen trophic cascades after predator losses[20], there were no interactive effects of MMEs on zooplankton biomass (two-way analysis of variance (ANOVA), predator removal × resource pulse; $F_{1,14} = 0.06$, $P = 0.82$; Fig. 1f), total primary production ($F_{1,14} = 0.49$, $P = 0.50$; Fig. 1g) or microalgal biomass ($F_{1,14} = 0.01$, $P = 0.93$; Fig. 1h) over time. Instead, food-web responses to MMEs were predicted by additive effects of predator removals and resource pulses on zooplankton biomass ($F_{1,14} = 5.59$, $P = 0.03$; $F_{1,14} = 0.62$, $P = 0.44$), total primary production ($F_{1,14} = 7.89$, $P = 0.01$; $F_{1,14} = 230.37$, $P < 0.01$) and microalgal biomass ($F_{1,14} = 3.97$, $P = 0.07$; $F_{1,14} = 0.70$, $P = 0.42$). This suggests that the effects of predator MMEs on trophic biomass over short timescales can be readily predicted by combining knowledge about how predator removals[4] and resource pulses[9] propagate through food webs in other systems. Below, we subsequently explore the mechanisms underlying zooplankton and microalgal dynamics after perturbations.

Community structural responses

Broad similarities in zooplankton and microalgal community structure after predator MMEs and predator removals indicated that structural changes were predominantly driven by predator and zooplankton consumer-mediated effects (Fig. 2, Extended Data Figs. 1 and 2 and Supplementary Table 1). Relative to the controls, both treatment conditions without predators had a higher biomass of key consumer competitors (Extended Data Fig. 3 and Supplementary Tables 1 and 2), including Cyclopoida (MMEs: +64%; predator removals: +88%), Daphniidae (MMEs: +231%; predator removals: +199%) and Bosminidae (MMEs: +53%; predator removals: +31%). Treatment conditions with resource additions had a higher biomass of other competitors

Article

with varied functional roles (Extended Data Fig. 3 and Supplementary Table 2), including Cyprididae (MMEs: +29%; resource pulses +28%) and Brachionidae (MMEs: +53%), the latter of which often proliferate alongside carrion additions[12,13]. Notably, our sampling approach prioritized enumerating large-bodied zooplankton that experience strong predator consumptive effects[22,23], which may have led to under-representation of some small rotifers and juvenile crustaceans (Methods). Despite this shortcoming, we still observed appreciable shifts in zooplankton composition and size, which often mediate ecological functional roles (Fig. 2). These shifts were probably attributable to altered competitive interactions[24,25] amid reduced predation, because predator losses led to a high biomass of omnivorous (such as Cyclopoida) and primarily herbivorous consumers (such as Daphniidae), as well as changes in production, because diverse competitor communities often proliferate after resource additions[12,13,24]. This increase in omnivorous consumers differentiated responses of MMEs and predator removals because the latter is initially expected to primarily increase herbivory[26].

Overall, biomass differences across trophic levels (Figs. 1 and 2, Extended Data Figs. 3 and 4 and Supplementary Tables 1–3) largely resulted from substantial density differences (Extended Data Figs. 1, 5 and 6 and Supplementary Tables 4 and 5) combined with modest differences in zooplankton body size (Fig. 2a, Extended Data Figs. 2 and 7 and Supplementary Table 6) and microalgal biovolume (Fig. 2b, Extended Data Figs. 2 and 8 and Supplementary Table 7). Planktivorous fish are well known to structure lake food webs by regulating zooplankton densities[12], and the mean zooplankton density increased in both treatment conditions without predators (MMEs: +34%; predator removals: +33%; Extended Data Fig. 5 and Supplementary Table 5). Planktivorous fish also exert selection on consumer body size[22], and both treatment conditions without predators had a larger mean zooplankton body size (MMEs: +14%; predator removals: +11%; Extended Data Fig. 2 and Supplementary Table 1), particularly among key consumer competitors after MMEs (Extended Data Fig. 7 and Supplementary Table 6). Comparatively, predator removals resulted in a larger mean body size of fewer key consumer competitors (Extended Data Fig. 7 and Supplementary Table 6) and a smaller mean body size of Brachionidae (−5%). This indicated that removing predators probably indirectly increased resource competition[12,13] after consumer densities increased (Figs. 1h and 2b), and zooplankton biomass simultaneously responded to both relaxation of size-selective predation[22] and temporary production enhancement[9] after the death and decomposition of predators, respectively. Thus, accounting for changes in body size (Fig. 2), which drive rapid ecological changes[25], could enhance forecasting community responses to MMEs.

Microalgal community responses to MMEs were also affected more by fish predator- and zooplankton-consumer-mediated effects rather than resource additions (Fig. 2b and Extended Data Figs. 2 and 4), which corroborates observations of fish MMEs in nature[27,28]. These effects were particularly evident several weeks after perturbations, when MMEs experienced sustained declines in production and microalgal biomass that were indicative of intensified herbivory[13,18] (Fig. 1i,j), but also consistent with reductions in predator-mediated nutrient cycling[29] (for example, excretion), and/or their combined effect[12,13] (for example, the dead fish paradox). Three lines of evidence suggest that intensified herbivory played the dominant role in this system.

First, MMEs and predator removals increased the mean biomass of key zooplankton competitors (Cyclopoida, Daphniidae; Fig. 2a, Extended Data Fig. 3 and Supplementary Table 2) that often have high consumption rates on phytoplankton[18]. Second, the mean biomass of green algae (Chlorophyta), which are frequently consumed by zooplankton[17–19], was low after predator removals (−42%, $t_{10.01} = -1.75$, $P = 0.08$; Extended Data Fig. 4 and Supplementary Table 3) and high after resource pulses (+11%, $t_{10.01} = 3.19$, $P < 0.01$). Moreover, both treatments without predators had a high mean biovolume of green algae (MMEs: +17%; predator removals: +23%; Fig. 2b, Extended Data Fig. 8

and Supplementary Table 7), which often attain a larger size through grazer-induced plasticity[30]. Third, resource pulses had a relatively high mean cyanobacteria biomass (+69%, $t_{22.1} = 2.05$, $P = 0.04$; Fig. 2b, Extended Data Fig. 4 and Supplementary Table 3) and density (+63%; $t_{21.86} = 1.93$, $P = 0.06$; Extended Data Fig. 6 and Supplementary Table 5), whereas MMEs had a relatively low mean cyanobacteria biomass (−48%, $t_{22.1} = -1.85$, $P = 0.07$) and density (−47%, $t_{21.86} = -1.68$, $P = 0.10$). This possible suppression of cyanobacteria differentiates microalgal responses to MMEs and resource pulses, and corroborates observations that zooplankton herbivory can facilitate recovery from cyanobacteria blooms[31].

Community biomass dynamics

Community trajectory analyses[32] indicated that MMEs generated unique community biomass dynamics through time compared with other perturbations (Fig. 3). Among zooplankton (Fig. 3a), MME dynamics were largely contained in community space occupied by smaller competitors; predator-removal dynamics occurred in space occupied by key competitors; and resource-pulse dynamics occurred in space occupied by smaller consumers with varied functional roles. Mean directed segment path dissimilarities (DSPD; Fig. 3b,e)—the relative distance in community space between treatments (that is, similarity in community composition)—also differed. Notably, zooplankton dynamics after MMEs were most like the controls (lowest DSPD in Fig. 3b), but dynamics after predator removals were most unlike the controls (highest DSPD in Fig. 3b). Similarly, predator removals exhibited the highest temporal stability in biomass among zooplankton groups (Fig. 3c) because lasting biomass shifts toward key competitors occurred (Fig. 3a and Extended Data Fig. 3). Lastly, zooplankton community dynamics after MMEs and resource pulses, but not predator removals, moved toward and ultimately converged with the control (Supplementary Table 8). Thus, in contrast to predator removals, enhanced production after MMEs weakened biomass shifts, even after fish predation was removed, as diverse consumers proliferated[12,13] (Extended Data Fig. 7). This maintenance of biomass among competitors probably resulted from novel ecological opportunities that arose in the aftermath of MMEs—namely enhanced productivity of phytoplankton resources amid decreased predation[24].

Compared with zooplankton, microalgal community dynamics were more similar across perturbations (Fig. 3d,e and Extended Data Figs. 2 and 6). The microalgal dynamics after MMEs were most like the controls (lowest DSPD in Fig. 3e), and the dynamics after predator removals were most unlike the controls (highest DSPD in Fig. 3e), similar to zooplankton. Biomass among microalgal groups exhibited similar temporal stability across perturbations (Fig. 3f), and dynamics after all perturbations moved towards and ultimately converged with the control (Supplementary Table 9). Thus, MMEs maintained biomass among a broad diversity of key consumers and exhibited minor changes in primary producer composition through time. This suggests that MMEs probably generated both influxes into green (autotrophic) food webs and, while not quantitatively explored here, brown (detrital) food webs, as decomposing predators generated appreciable periphyton (Fig. 1b). Theory suggests that influxes into both green and brown food webs can increase ecosystem stability because both consumers and decomposers enhance community resiliency[33,34]. Conversely, MMEs may also destabilize communities if nutrients are not readily converted into producer biomass[8].

Considerable work has focused on how predator losses destabilize food webs through long-term shifts in consumer and producer biomass[4,6,35]. Yet understanding how communities are restructured after predator losses may be critical for resolving their short- and long-term effects[36,37]. Predator removal conditions, which had high consumer densities (Extended Data Figs. 1 and 5) and no resource additions (Fig. 1), generated lasting shifts in consumer biomass (Fig. 2a and
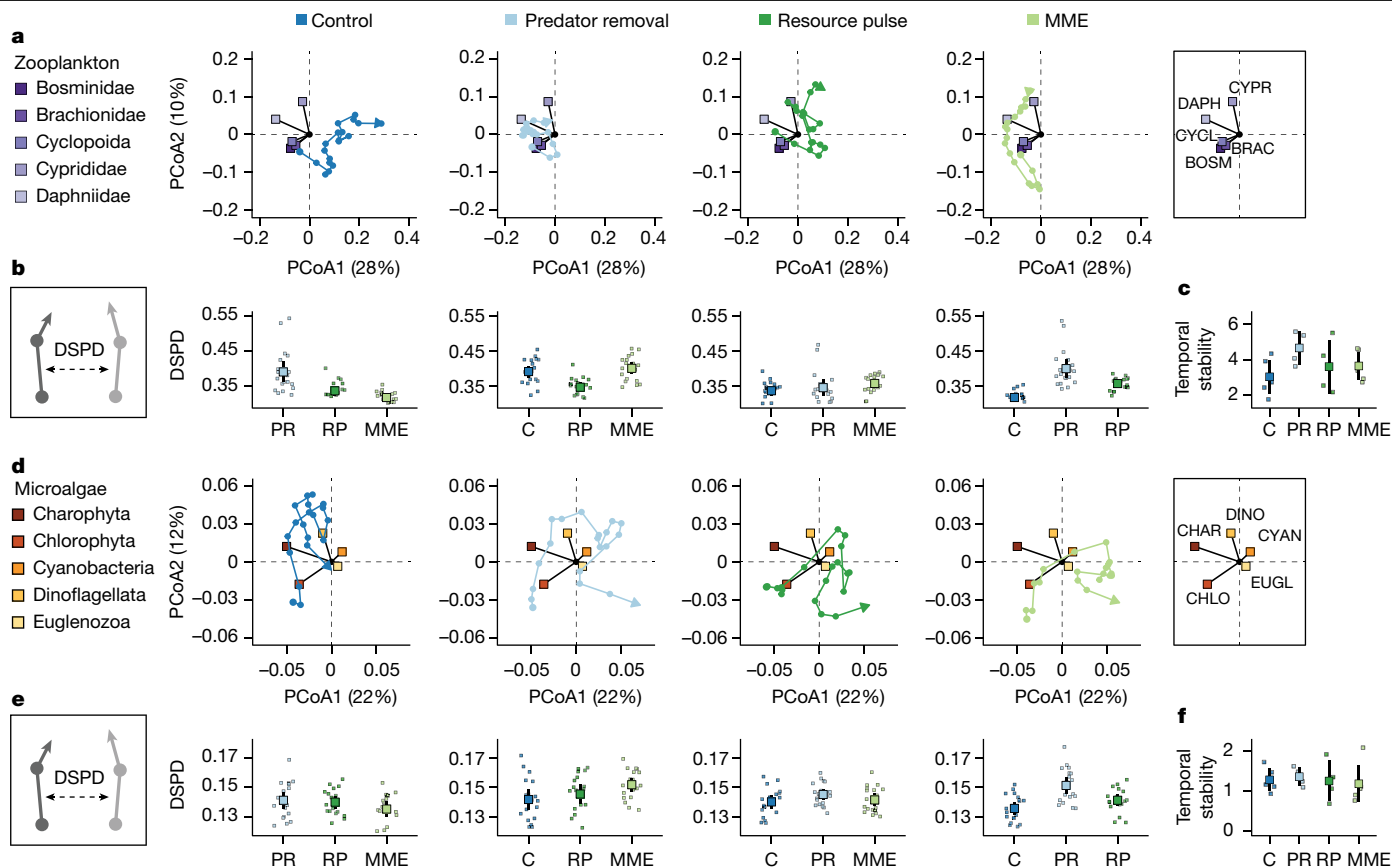
Fig. 3 | Distinct zooplankton and microalgal community biomass trajectories after predator removals, resource pulses and MMEs. a,d, Ecological trajectory analyses of zooplankton (**a**) and microalgal (**d**) biomass dynamics in the predator removal (light blue, PR), resource pulse (dark green, RP), MME (light green) and the control (C; dark blue) scenarios. Trajectories show smoothed moving averages. Connected dots represent sample periods and arrows emphasise the final sample period. Principal coordinate analysis (PCoA) loadings of zooplankton and phytoplankton are shown by purple and orange squares, respectively. Insets show loading positions. **b,e**, The mean DSPDs and 95% CIs (squares and lines, respectively). This metric represents the average distance between the focal trajectory and a comparison trajectory during the same sample periods (as illustrated by the small insets on the left) for zooplankton (**b**) and microalgae (**e**). **c,f**, The temporal stability (temporal mean/temporal s.d.) and 95% CIs (squares and lines, respectively), for the biomass of zooplankton (**c**) and microalgae (**f**). Data were analysed from 228 biologically independent samples for DSPD estimates (**b** and **e**; n = 57 for each treatment) from one experiment. Data were analysed from 18 samples (**c** and **f**) for the control (n = 5), predator removal (n = 4), resource pulse (n = 4) and MME (n = 5) scenarios from one experiment. Statistical analysis was performed using a GAMM (**a**–**c**) and two-sided two-way ANOVA (**d**–**f**).

Extended Data Fig. 3). Comparatively, only MMEs maintained appreciable biomass among various community members (Fig. 2a) while exhibiting consumer and primary producer biomass dynamics that ultimately converged with undisturbed systems (Supplementary Tables 8 and 9). This indicated greater productivity and functional diversity probably led to weakened biomass shifts among key competitors after predator losses, which corroborates expectations based on the productivity–stability[38] and diversity–stability hypotheses[39]. Paradoxically, these properties also indicate that the ecological aftermath of MMEs may be cryptic in nature[37], potentially leading to underestimations of their occurrence and effects over short timescales.

The roles of top-down and bottom-up effects in shaping communities have influenced ecology for over 50 years[1–3,14,15]. Our study shows that predator MMEs generate trophic biomass responses that can be predicted by integrating classic theory on top-down and bottom-up regulation[8], yet exhibit distinct food web dynamics and community structure that cannot be readily predicted by integrating these ideas. It is notable that the effects of MMEs cannot be predicted by only removing predators. Indeed, our results indicate that the effects of trophic downgrading in the immediate aftermath of MMEs might be thought of as 'trophic decoupling'. During this shuffling of the food web, the effects of predators were initially decoupled from lower trophic levels, but their biomass was later assimilated by producers and subsequently passed upwards. Predator mortalities can therefore generate direct bottom-up effects in ecosystems that may facilitate their eventual recovery. Future studies may be able to anticipate ecological outcomes of these and other increasingly common ecological catastrophes[7,11] by similarly synthesizing foundational concepts formulated in a less volatile world.

Online content

Any methods, additional references, Nature Portfolio reporting summaries, source data, extended data, supplementary information, acknowledgements, peer review information; details of author contributions and competing interests; and statements of data and code availability are available at https://doi.org/10.1038/s41586-023-06931-7.

1. Hairston, N. G., Smith, F. E. & Slobodkin, L. B. Community structure, population control, and competition. *Am. Nat.* **94**, 421–425 (1960).
2. Paine, R. T. Food web complexity and species diversity. *Am. Nat.* **100**, 65–75 (1966).
3. Paine, R. T. Food webs: linkage, interaction strength and community infrastructure. *J. Anim. Ecol.* **49**, 666–685 (1980).
4. Estes, J. A. et al. Trophic downgrading of planet Earth. *Science* **333**, 301–306 (2011).
5. Myers, R. A. & Worm, B. Rapid worldwide depletion of predatory fish communities. *Nature* **423**, 280–283 (2003).
6. Dirzo, R. et al. Defaunation in the Anthropocene. *Science* **345**, 401–406 (2014).

Article

7. Fey, S. B. et al. Recent shifts in the occurrence, cause, and magnitude of animal mass mortality events. *Proc. Natl Acad. Sci. USA* **112**, 1083–1088 (2015).

8. Fey, S. B., Gibert, J. P. & Siepielski, A. M. The consequences of mass mortality events for the structure and dynamics of biological communities. *Oikos* **128**, 1679–1690 (2019).

9. Polis, G. A., Anderson, W. B. & Holt, R. D. Toward an integration of landscape and food web ecology: the dynamics of spatially subsidized food webs. *Annu. Rev. Ecol. Syst.* **28**, 289–316 (1997).

10. Hamilton, S. L. et al. Disease-driven mass mortality event leads to widespread extirpation and variable recovery potential of a marine predator across the eastern Pacific. *Proc. R. Soc. B* **288**, 20211195 (2021).

11. Tye, S. P. et al. Climate warming amplifies the frequency of fish mass mortality events across north temperate lakes. *Limnol. Oceanogr. Lett.* **7**, 510–519 (2022).

12. Threlkeld, S. T. Planktivory and planktivore biomass effects on zooplankton, phytoplankton, and the trophic cascade: fish effects on plankton. *Limnol. Oceanogr.* **33**, 1362–1375 (1988).

13. Vanni, M. J. & Findlay, D. L. Trophic cascades and phytoplankton community structure. *Ecology* **71**, 921–937 (1990).

14. Leopold, A. *A Sand County Almanac* 129–133 (Random House, 1949).

15. Schindler, D. W. Eutrophication and recovery in experimental lakes: implications for lake management. *Science* **184**, 897–899 (1974).

16. Vitousek, P. M. Beyond global warming: ecology and global change. *Ecology* **75**, 1861–1876 (1994).

17. Bergquist, A. M. & Carpenter, S. R. Limnetic herbivory: effects on phytoplankton populations and primary production. *Ecology* **67**, 1351–1360 (1986).

18. Hansen, P. J., Bjørnsen, P. K. & Hansen, B. W. Zooplankton grazing and growth: Scaling within the 2–2,000-μm body size range. *Limnol. Oceanogr.* **42**, 687–704 (1997).

19. Porter, K. G. Selective grazing and differential digestion of algae by zooplankton. *Nature* **244**, 179–180 (1973).

20. Su, H. et al. Determinants of trophic cascade strength in freshwater ecosystems: a global analysis. *Ecology* **102**, e03370 (2021).

21. Boros, G., Takács, P. & Vanni, M. J. The fate of phosphorus in decomposing fish carcasses: a mesocosm experiment. *Freshw. Biol.* **60**, 479–489 (2015).

22. Brooks, J. L. & Dodson, S. I. Predation, body size, and composition of plankton: the effect of a marine planktivore on lake plankton illustrates theory of size, competition, and predation. *Science* **150**, 28–35 (1965).

23. Galbraith, M. G. Size-selective predation on daphnia by rainbow trout and yellow perch. *Trans. Am. Fish. Soc.* **96**, 1–10 (1967).

24. DeMott, W. R. & Kerfoot, W. C. Competition among cladocerans: nature of the interaction between bosmina and daphnia. *Ecology* **63**, 1949 (1982).

25. Gibert, J. P., Han, Z. Y., Wieczynski, D. J., Votzke, S. & Yammine, A. Feedbacks between size and density dependence determine rapid eco-phenotypic dynamics. *Funct. Ecol.* **6**, 1668–1680 (2022).

26. Borer, E. T. et al. What determines the strength of a trophic cascade? *Ecology* **86**, 528–537 (2005).

27. Vanni, M. J. et al. Effects on lower trophic levels of massive fish mortality. *Nature* **344**, 333–335 (1990).

28. Nagdali, S. S. & Gupta, P. K. Impact of mass mortality of a mosquito fish, Gambusia affinis on the ecology of a fresh water eutrophic lake (Lake Naini Tal, India). *Hydrobiologia* **468**, 45–52 (2002).

29. Vanni, M. J. Nutrient cycling by animals in freshwater ecosystems. *Annu. Rev. Ecol. Syst.* **33**, 341–370 (2002).

30. Van Donk, E., Ianora, A. & Vos, M. Induced defences in marine and freshwater phytoplankton: a review. *Hydrobiologia* **668**, 3–19 (2011).

31. Conley, D. J. et al. Controlling eutrophication: nitrogen and phosphorus. *Science* **323**, 1014–1015 (2009).

32. De Cáceres, M. et al. Trajectory analysis in community ecology. *Ecol. Monogr.* **89**, 1–20 (2019).

33. Mougi, A. Coupling of green and brown food webs and ecosystem stability. *Ecol. Evol.* **10**, 9192–9199 (2020).

34. Rooney, N., McCann, K., Gellner, G. & Moore, J. C. Structural asymmetry and the stability of diverse food webs. *Nature* **442**, 265–269 (2006).

35. Fricke, E. C. et al. Collapse of terrestrial mammal food webs since the Late Pleistocene. *Science* **377**, 1008–1011 (2022).

36. Pimm, S. L. The complexity and stability of ecosystems. *Nature* **307**, 321–326 (1984).

37. Ives, A. R. & Cardinale, B. J. Food-web interactions govern the resistance of communities after non-random extinctions. *Nature* **429**, 174–177 (2004).

38. MacArthur, R. Fluctuations of animal populations and a measure of community stability. *Ecology* **36**, 533–536 (1955).

39. McCann, K. S. The diversity–stability debate. *Nature* **405**, 228–233 (2000).

Methods

Experimental design

Our main goal was to experimentally compare ecological dynamics in tritrophic freshwater food webs (phytoplankton producers, zooplankton consumers and fish predators) after three different ecological perturbations: predator removals (that is, top-down effects are manipulated), resource pulses (that is, bottom-up effects are manipulated) and predator MMEs (that is, both top-down and bottom-up effects are manipulated, hereafter MMEs). We specifically aimed to compare these perturbations to an undisturbed experimental control (that is, no manipulation of top-down or bottom-up effects) and make comparisons among different perturbations. In this study, we experimentally induced mortalities of only predators (see the 'Freshwater mesocosms' section). This kind of mortality event exemplified a single-trophic-level MME, such as might occur during a disease outbreak—the leading cause of MMEs in freshwater fish[7,11]. In nature, MMEs can be driven by many biotic and abiotic factors, as well as affect numerous trophic levels simultaneously[7,11].

We focused these inquiries on tritrophic food web responses within freshwater lake communities for several reasons. First, phytoplankton, zooplankton and planktivorous fish constitute major food web components in freshwater lake systems[40]. Second, freshwater lake systems have well-understood trophic links, such as between planktivorous fish and herbivorous zooplankton[12,13,17–19,22,24]. Third, freshwater lake systems frequently experience fish MMEs[7,11], and fish carrion rapidly decomposes and remineralizes within lentic systems[12,13,21,27,28]. Moreover, fish MMEs in nature rapidly generate temporary increases in total productivity[27] owing to rapid increases in limiting nutrient concentrations as fish carrion decomposes[28]. Fourth, the addition and/or removal of fish predators and resources rapidly alters zooplankton and phytoplankton community structure[12,13]. Fifth, ecological dynamics of freshwater lake communities can be coarsely approximated using smaller-scale experimental mesocosms[41,42]. Lastly, mesocosms that mimic major biological conditions of lakes can, in contrast to whole-lake manipulations and natural observations, be replicated and controlled[41,42]. Mesocosms are therefore amendable and ideal for studying extreme events in nature, such as MMEs affecting wild populations[27,28].

To understand how perturbations affected different trophic levels and major functional groups, we used a sampling approach that aimed to efficiently collect and enumerate key consumer and producer groups at coarse taxonomic scales of family and phyla, respectively, within mesocosms and through time (see the 'Freshwater mesocosms' section). We used this approach because it allowed for the time-efficient enumeration of focal consumers and producers, as well as the robust estimation of key traits that underlie consumer–resource interactions, such as body size or volume[25], using a combination of historical and modern methods described below. Moreover, these body measurements may be used alongside density estimates to approximate biomass through length–weight[43,44] and volume–biomass[45,46] equations, respectively. Future studies with sampling approaches that obtain higher taxonomic resolution data are necessary to address questions about how individual species are affected by the perturbations induced in this study.

Importantly, recent theory predicts that predator MMEs simultaneously generate top-down and bottom-up forces, and thereby exhibit distinct temporal ecological dynamics that cannot be explained solely by the independent effects of predator removals or resource pulses[8]. We therefore conducted a mesocosm experiment with a 2 × 2 factorial design (Fig. 1a; five replicates each) by manipulating the presence/absence of live fish predators and the presence/absence of dead fish predators (that is, fish carrion) to create three different ecological perturbations and an experimental control. These perturbations included predator removals (ten live fish absent, dead fish absent), resource pulses (ten live fish present, ten dead fish added) and predator MMEs (live fish absent, ten dead fish added), in addition to an undisturbed control treatment (ten live fish present, dead fish absent).

We prepared 20 mesocosms by sequentially adding trophic levels over 5 weeks; waiting three weeks; removing all fish (bluegill; *Lepomis macrochirus*) predators across mesocosms to induce similar perturbations and perform fish euthanasia through approved procedures (IACUC, 191060); and inducing treatments with live and euthanized fish (Fig. 1b). We then extensively monitored larger-bodied zooplankton communities, microalgal communities (that is, phytoplankton within the size range of 2–100 μm that are readily consumed by common zooplankton[17–19]) and total production (chlorophyll *a*) for 120 days. This experimental duration encompassed the timespan that limiting nutrient concentrations (that is, N, P) are elevated and diminish after experimentally induced bluegill mortalities in similarly sized mesocosms[21]. We checked mesocosms approximately daily for inadvertently dead bluegill to the best of our ability and, when necessary, replaced each with a similarly sized live bluegill. We later excluded one replicate each from the predator removal and resource pulse treatments because frogs deposited eggs and a *Euglena* algal bloom occurred, respectively. Thus, there were five mesocosm replicates for the MME and control treatments, and four mesocosm replicates for the predator-removal and resource-pulse treatments.

Freshwater mesocosms

We arranged 20 mesocosms (1,000 l, 1.61 m × 1.75 m × 0.64 m) in a 2 × 10 matrix at an outdoor facility at the University of Arkansas, Fayetteville, USA. Each mesocosm was filled with 750 l of low-nutrient tap water that was allowed to dechlorinate for 1 week. We added ten partially unravelled strands of 0.91 m × 0.95 cm polyester rope weighted down by a cinderblock to the same quadrant of each mesocosm to serve as underwater refugia for fish and zooplankton. Each mesocosm was covered with 1 mm plastic mesh to hinder introduction of non-target taxa, as well equipped with a plastic tarp that was used to cover mesocosms when heavy precipitation occurred to help mitigate substantial water level changes. We obtained leaf litter from deciduous forests surrounding Lake Wilson, Arkansas, USA (35.999387°, −94.136369°, WGS84) and dried it for 1 week, after which we added 500 g of dried leaf litter to each mesocosm for an initial nutrient source and microbial detritivore community.

After 1 week, we inoculated each mesocosm with local phytoplankton communities through around 189 l of filtered lake water (125 μm sieve) obtained from the littoral zone of Lake Wilson, Arkansas. We then allowed phytoplankton communities to proliferate for 2 weeks before adding zooplankton. We collected zooplankton from the littoral zone of Lake Wilson, Arkansas, USA at day (approximately 0.5 m depth) and night (< 1 m depth) through a 50 μm mesh net. Lake Wilson is a low-productivity lake with low chlorophyll *a* (~3.7 μg l^{-1}) and zooplankton densities (around 59 individuals per l) over recent surveys. We removed insect taxa from each zooplankton sample and then consolidated zooplankton samples in a separate 1,000 l mesocosm that was assembled as described above. This sample consolidation process was necessary to acquire adequate zooplankton abundances for stocking mesocosms at target densities. After collecting zooplankton for 2 weeks, we passed the consolidated zooplankton samples through a 50 μm sieve and aliquoted filtered samples into 20 subsamples that contained around 200 individuals, to mimic near natural densities, of each locally dominant zooplankton family: Brachionidae, Bosminidae, Cyclopoida, Cyprididae and Daphniidae. We focused on these zooplankton families because they often experience varying levels of fish predation[12,13,22,23,47], and have available length–weight biomass equations that span the range of expected body sizes for most adults[43,44]. Moreover, the range of body sizes applicable to these equations spans the range of expected adult body sizes of the focal taxa[12,13,22].

We allowed zooplankton communities to proliferate for 10 days before adding 10 live bluegill of similar length (mean = 7.15 cm;

Article

s.d. = 0.33 cm). Bluegill were about or less than 1 year old, mostly male individuals, and obtained from the Arkansas Department of Game and Fish, to each mesocosm. Bluegill are common planktivorous fish that act as keystone predators in littoral communities[48] and exhibit size-selective predation on zooplankton[49]. To ensure that all mesocosms initially experienced similar ecological dynamics, we maintained tritrophic food webs across mesocosms for 3 weeks before inducing treatments (that is, perturbations). Next, we used an electroshocker to remove all fish from all mesocosms. We administered the electroshocker to all mesocosms to remove all fish so that there were no potential effects of electroshocking-specific treatments and so that all community members within mesocosms (that is, producers, consumers) were equally affected. We next performed euthanasia by rapid chilling for at least 1 h (-2–4 °C) and then freezing fish (for those assigned to predator mortalities) for at least 24 h (IACUC, 191060). This euthanasia method helped to avoid potential confounding factors from chemical-based euthanasia approaches[50]. Moreover, our use of predator carrion as the resource addition enabled the stoichiometry of the resource pulses and influx of resources during the MME to be held constant. The next day, we used additional live bluegill, which were housed in non-experimental mesocosms, and euthanized bluegill, obtained from the above procedure, to induce treatments. Researchers were aware of which bluegill were placed in each replicate (that is, there was no blinding). Treatments were randomly assigned to mesocosms (*n* = 5 per treatment) using a random number generator.

Sample collection

We were specifically interested in understanding whether predator removals, resource pulses and predator MMEs generated disparate responses through trophic biomass, community structure, functional trait composition and transient community dynamics. To make comparisons between these aspects of food web dynamics, we extensively monitored zooplankton communities, microalgal communities and total production over the entire experimental duration.

As recent theory suggests predator MMEs generate transient dynamics that are distinguishable from dynamics expected from independent effects of predator removals or resource pulses[6], we used a high-intensity sampling regime to capture transient dynamics of zooplankton communities, microalgal communities and chlorophyll *a* that may differentiate these perturbations. This sampling regime involved two different sampling intensities over the experimental duration: once per week for the first 3 weeks (that is, before treatments were induced), then twice per week for 5 weeks, then once per week for an additional 10 weeks. For each sampling effort, we collected zooplankton and phytoplankton samples over three consecutive days. This staggered sampling regime was necessary due to logistical constraints and involved acquiring phytoplankton samples over two consecutive days and zooplankton samples over one separate day for each respective sampling period. We used these samples to estimate total production (chlorophyll *a*) and enumerate characteristics of zooplankton and microalgal communities. We identified zooplankton to family and microalgae to phyla, which correspond to major functional groups for freshwater consumers and producers, respectively[51,52].

For chlorophyll *a* estimates, we used a standard and widely adopted fluorescence-based alcohol-digestion approach[53,54]. From each mesocosm on each sampling date, two 50 ml subsamples were passed through 47 mm wide nylon filters with 0.22 μm perforations (AllPure Biotechnology), placed in separate scintillation tubes with 4 ml of 95% ethanol and refrigerated (-2–4 °C) for 24 h. We used nylon filters because they have been shown to provide more consistent, repeatable chlorophyll *a* estimates than traditional glass filters due to their higher retention of chlorophyll *a*[55]. We then used a fluorometer (Trilogy, Turner Designs), which we standardized before use with a known concentration of chlorophyll *a*, to quantify chlorophyll *a* from both samples: the mean value was used in all analyses. Although fluorescence of the chlorophyll *a* degradation product pheophytin *a* can generate bias by overestimating chlorophyll *a* concentrations by approximately 10% (refs. 56,57), the highly selective optical filters used in this fluorometric method minimize these interferences[54]. We did not monitor limiting nutrient concentrations. However, a study with similar mesocosms has demonstrated that both dissolved nitrogen and phosphorus concentrations are rapidly elevated after bluegill decomposition, especially several weeks after adding carcasses[21].

To quantify microalgal community structure, we examined a portion of the remaining water sample using fluid imaging (FlowCAM VS-Series, Fluid Imaging). To perform fluid imaging, we first passed each water sample through a 125 μm sieve and homogenized them, after which a 2 ml subsample was placed through a 100 μm × 1 mm FlowCell (Fluid Imaging). This sample volume is commonly used to enumerate phytoplankton communities from various environments, ranging from microcosms[58] to large freshwater lakes[59]. In this study, FlowCam settings included an AutoImage rate of 20 fps and flow rate of 0.170 ml min^{-1}. These settings were similar to previous studies that used fluid imaging to enumerate phytoplankton[58], and resulted in a 23.4% efficiency rate per sample. Efficiency rate is the percentage of fluid volume imaged relative to the total sample volume processed, and an efficiency under 70% ensures repeated pictures of the same particles are not captured. We used VisualSpreadsheet (v.4) to examine and classify microalgal taxa. Specifically, we post hoc examined all images from every fifth sample from each mesocosm to create image libraries of dominant microalgal genera. We then manually examined all images acquired from each 2 ml sample; assigned all images of living microalgae to genera; and categorized genera by phylum as follows: Charophyta (*Cosmarium*, *Mougeotia*, *Staurastrum*), Chlorophyta (*Ankistrodesmus*, *Closteriopsis*, *Closterium*, *Coelastrum*, *Crucigenia*, *Franceia*, *Oocystis*, *Scenedesmus*), Cyanobacteria (*Anabaena*), Dinoflagellata (*Gymnodinium*), Euglenozoa (*Euglena*). We identified 28,161 microalgae to phylum for analyses (mean = 68 individuals per sample, s.d. = 211 individuals per sample).

As we were interested in understanding how perturbations affected microalgal community dynamics through time, we next used fluid imaging data to enumerate microalgal biomass, density and biovolume (area-based volume) through time. For microalgal density estimates, we converted abundance estimates of each microalgal phylum and across phyla from each fluid imaging sample (2 ml) to natural log-transformed density per L. For microalgal biovolume estimates, we used the area-based volume of each microalgae individual and the FlowCam VS-Series image scaling factor (0.56) to estimate the mean biovolume of each phylum and across phyla for each sample. Specifically, we used the mean area-based volume in volume–biomass equations of congener microalgae[45,46] to estimate the biomass of each microalgal individual. We used these data to calculate the natural-log-transformed biomass per litre of each phylum and across phyla. We included all individual microalgae that were assigned to phyla when calculating density, biovolume and biomass estimates. These microalgal density and biomass estimates were similar to comparable estimates in previous studies with similar fluid imaging equipment[58]. We considered chlorophyll *a* to be an indicator of total primary production minus herbivory, or the amount of resources available during a sample period, and microalgal biomass to be an indicator of the availability of key resources to consumers.

We also quantified zooplankton biomass, density and body size through time. To acquire zooplankton samples, we lightly mixed each mesocosm using a perforated Secchi disk (-20 cm diameter), allowed the disturbed leaf litter to settle and placed an integrated tube sampler (-5 cm diameter, -91 cm length) through the water column. We used standardized measurements on the side of the integrated tube sampler to measure the water level of each mesocosm to improve estimates of mesocosm water volume when samples were acquired, and therefore zooplankton density estimates, through time. All zooplankton samples

were collected from the same quadrant across mesocosms. We passed zooplankton samples through a 125 μm sieve and placed samples in Lugol's iodine solution for preservation and to aid visual identification. We used this pore size to provide reliable and robust information about dynamics of medium to large-bodied zooplankton, though at the potential cost of underrepresenting certain small zooplankton, such as juvenile crustaceans and rotifers[60]. Large-bodied zooplankton taxa often exhibit high consumption rates of algae[18], and *L. macrochirus* is known to exhibit size-selective predation of large-bodied zooplankton[49]— factors that probably strongly influence community responses to the manipulation of abundances of predators and/or resources based on existing knowledge of trophic links[12,13,17–19,22,24]. Future studies would benefit from examining a broader range of zooplankton size classes, as well as larger volumes of water when assessing microalgal communities, to understand additional ecological responses to this set of perturbations.

After collecting all of the zooplankton samples, we used light microscopy (×20; Leica Camera Model EC4) to identify and measure the body sizes of dominant zooplankton families: Bosminidae (*Bosmina*), Brachionidae (*Brachionus*), Cyclopidae (*Cyclops*), Cyprididae (*Cypridopsis*) and Daphniidae (*Daphnia*). On average, we counted around 53.9 individuals per sample to family for abundance estimates (s.d. = 19.4 individuals per sample). These individuals were obtained from samples (through the integrated tube sampler) with water volumes that ranged from around 0.74 l to 1.1 l. We also measured body sizes of ten haphazardly selected individuals (or all individuals if there were less than ten) for each zooplankton family from each sample. We used the mean body size of each zooplankton family and sample period to estimate mean zooplankton biomass through length–weight regressions for Bosminidae[43], Brachionidae[43], Cyclopidae[43], Cyprididae[43] and Daphniidae[44]. We used these data to calculate the natural-log-transformed biomass per litre of each zooplankton family and across families. Lastly, we converted abundances of each zooplankton family and across families to natural-log-transformed density per litre. On average, we measured body size of around 19.7 individuals per family per sample (s.d. = 2.68 individuals per sample). We included all individual zooplankton that were assigned to family when calculating density, body size and biomass estimates.

Although multiple traits shape food web dynamics, we focused on one shared trait—overall size—to understand the functional trait response of microalgae and zooplankton and, therefore, consumer–resource interactions, for several reasons. First, we measured microalgal body volume and zooplankton body size because these body measurements are central functional traits mediating consumer–resource interactions in freshwater systems[18,19,22,61]. Second, body size shapes metabolic rates that influence many biological processes[62], as well as how organisms interact within food webs[63,64]. Third, size measurements are commonly recorded traits that often correlate with other functional traits associated with ecological processes (that is, respiration rates, foraging rates, mortality rates)[63]. Lastly, body measurements allowed for quantification of zooplankton and microalgal biomass through the regression-based approach described above.

After collecting and enumerating all samples, we used linear mixed models to compare average chlorophyll *a*, microalgal biomass and zooplankton biomass estimates during the first three sample periods to determine whether mesocosms had a similar community structure before treatments were induced. These models used the raw (non-smoothed) data and had the form: biomass estimates ~ treatment with a nested random effect of sampling period and mesocosm. There were no differences in chlorophyll *a*, microalgal biomass and zooplankton biomass between treatments during the first three sample periods (Extended Data Fig. 9).

We next calculated smoothed moving averages of chlorophyll *a*, zooplankton community characteristics (biomass, density, body size), microalgal community characteristics (biomass, density, biovolume).

We used this smoothing method, described below, to reduce the propagation of sampling error into temporal variation (for example, slightly weaken large increases and decreases between adjacent sample periods). Smoothing has become a widely adopted approach for time-series data[65,66], and there are many different types of smoothing approaches[65–68]. The approach used here involved calculating smoothed moving averages over three adjacent sample periods (that is, a focal, previous and subsequent sample period), with the focal sample period being weighted more than the previous and subsequent sample periods. These weights were 1 for the focal sample period and 1/3 for the other periods. Notably, this approach led to the first and last sample periods being excluded from the smoothed data, as they did not have a previous or subsequent sample period, respectively, for the necessary calculations. We used smoothed data at the replicate level for all statistics except for community trajectory analyses, described below, because associated statistical tests involved pairwise comparisons and thus treatment-level data (that is, averaged by treatment) addressed more intuitive and informative questions.

Statistical analyses
We used three statistical approaches to compare ecological dynamics after perturbations. First, we used two-sided, two-way ANOVA to understand whether MMEs exhibited additive or non-additive (that is, synergistic or antagonistic) effects of predator removals and resource pulses on trophic biomass. This was possible because treatments included all combinations of these two factors: (1) predator removals (both fish and carrion absent); (2) resource pulses (both fish and carrion present); (3) MMEs (fish absent, carrion present); and (4) a control treatment (fish present, carrion absent). These models had the form: response ~ predator removal × resource pulse with a nested random effect of sampling period and mesocosm. We used trophic biomass (chlorophyll *a*, zooplankton biomass or microalgal biomass) as the response variable. For the reference groups, we considered fish present (that is, the absence of a predator removal) and predator carrion absent (that is, the presence of a resource pulse), as provided in the control treatment.

If present, we considered a significant interaction to be indicative of non-additive (that is, interactive) effects MMEs on trophic biomass over the entire experimental duration that would not be readily predicted by the simple additive effects (that is, only independent effects) of predator removals and resource pulses. To evaluate the robustness of this core analysis to our smoothing approach, we performed models as described above but with the raw (that is, non-smoothed) data. These models had the same form as above: response ~ predator removal × resource pulse with a nested random effect of sampling period and mesocosm. These models (Extended Data Fig. 10) generated nearly identical findings as described in the main text (Fig. 1).

Second, we used general additive mixed models[69] (GAMMs) to understand whether disturbances generated disparate responses in zooplankton and microalgal communities through time. These models had biomass, density and individual body size or biovolume of trophic levels (that is, chlorophyll *a*, zooplankton or microalgae) or functional groups (that is, zooplankton family or microalgal phyla) as separate response variables. All GAMMs had a gamma error distribution with a log link, except for models with zooplankton body size because they did not require log transformations. For each response variable, we used the Akaike information criterion (AIC) to compare five GAMM forms (Supplementary Table 9) that allowed for different or similar shapes, different or similar intercepts and the presence/absence of a smoothing penalization on the time effect. We considered a delta-AIC of <2 to be significant for comparisons among these model forms, which included fixed effects of treatment, sample or both treatment and sample, as well as the presence/absence of a smoothing penalization on the time effect. For these models, we used treatment as the predictor variable with the control treatment as the reference group,

rather than predictor variables of predator removal × resource pulse as in the first approach, so that there were treatment-specific temporal smoothing penalizations.

After this first step in model selection, 29 out of 34 models (Supplementary Table 10) were best explained with temporal smoothing penalization (that is, models 4–5 in Supplementary Table 9). The five remaining models (Supplementary Table 4) were best explained without temporal smoothing penalization (that is, models 1–3 in Supplementary Table 3), as there were similar fits for model forms with or without such penalization. We next performed additional model selection on the first group of models to obtain the best penalization parameter and account for correlation of autoregressive moving averages by auto-regressive moving average using the nlme package[70]. We used AIC to compare six dimensions (k; 3, 5, 8, 10, 12 and 15), which encompassed the full range of possible dimensions, for the smooth term for each model through penalized spline regressions in the mgcv package[71]. The final form of each GAMM is listed in Supplementary Table 4. For all GAMMs, we considered differences in intercepts (that is, parametric coefficients of treatments and corresponding t values) to indicate differences in mean responses, and differences in model shape (that is, treatment-specific time effect) to indicate whether treatments had different trajectories, compared with the control. For brevity, we discuss only differences in intercepts for GAMMs in the main text. We used this GAMM-based approach for all biomass, density and body size or biovolume responses except for biovolume of three microalgal phyla (Cyanobacteria, Dinoflagellata and Euglenozoa), which were too variable within and across mesocosms for meaningful inferences and, therefore, only summarized for descriptive purposes (Fig. 2b). Complete details about GAMMs are shown in Supplementary Table 1 for trophic biomass estimates, Supplementary Table 2 for zooplankton biomass estimates, Supplementary Table 3 for microalgal biomass estimates, Supplementary Table 4 for zooplankton density estimates, Supplementary Table 5 for microalgal density estimates, Supplementary Table 6 for zooplankton body size estimates and Supplementary Table 7 for microalgal biovolume estimates.

Third, we used communities trajectory analyses[32,72] to compare the ordination of zooplankton and microalgal community biomass dynamics after perturbations. This recently developed approach can be used to examine and compare dynamics of biological systems (for example, communities) using PCoA. In this approach, experimental units (mesocosms with different perturbation treatments in this case) are tracked through time and differences in temporal dynamics are quantified by their position along axes describing community composition (that is, PCoA loadings of different taxonomic groups). To compare biomass dynamics after perturbations and obtain intuitive results from statistical tests associated with this approach, two standard data adjustments were necessary. First, community trajectory analyses require data continuity, and there were samples in which some microalgal phyla, especially Cyanobacteria and/or Euglenozoa, were not observed. Thus, to account for this lack of information and ensure data continuity without distorting trends, we added the minimum observed biomass and density (across all mesocosms and samples) to each microalgal phyla biomass and density estimate before performing analyses. Second, we used smoothed data at the treatment level rather than at the replicate level for this set of analyses because the associated statistical tests compare aspects of community trajectories through pairwise comparisons. Thus, treatment-level data allowed for direct comparisons of community biomass dynamics between treatments. We next determined the most appropriate ordination approach separately for biomass among zooplankton groups and biomass among microalgal groups by comparing Euclidean distances of each set of biomass estimates through time to several dissimilarity indices, including Bray–Curtis, local transformation, square root, metric multidimensional scaling and non-metric multidimensional scaling. We used local transformations because they provided the lowest stress levels[73] (>0.2), passed the triangle inequality, and are recommended to limit distortion and aid interpretability of community trajectories[32].

After determining the appropriate transformation for models, we then compared two characteristics of biomass dynamics (that is, trajectories) between treatments. First, we calculated mean DSPDs (Fig. 3b,e) for each pairwise comparison between treatments. This metric represents the average distance between segment midpoints of different trajectories in community ordination space at comparable sample periods, or how different communities are in overall ordination space. We were therefore able to use this metric to understand whether specific perturbations generated community biomass dynamics that were similar (low DSPD) or dissimilar (high DSPD) to other perturbations, as well as whether perturbations generated biomass dynamics that were similar or dissimilar to the control. We therefore considered the lowest mean DSPD among perturbations, compared with the control, to indicate which perturbation generated biomass dynamics that were most similar to dynamics after the control treatment and through time.

For the second trajectory metric, we compared the ending directions of different trajectories, or whether trajectories converged or diverged through time, using Mann–Whitney U-tests in the ecotraj package[32]. These asymmetric convergence/divergence tests involved pairwise comparisons that determined whether different combinations of treatment-level trajectories (as shown in each column of Fig. 3a,d) moved toward (that is, converge) or away from (that is, diverge) each other through time[32] (Supplementary Tables 8 and 9). Specifically, this involved pairwise comparison tests that examined whether the distance between a focal trajectory and a comparison trajectory became smaller (convergence) or larger (divergence) through time. We used that approach for this study to specifically determine whether perturbations converged or diverged with the control. Each pairwise comparison between treatments provided a single tau statistic (τ) that was bounded by −1 and 1, such that negative and positive values indicated divergence or convergence from the focal trajectory toward the comparison trajectory.

To complement comparisons of these two community trajectory characteristics by treatment, we calculated one additional metric with the same community biomass data (that is, averaged by treatment). This metric, temporal stability[74], is used to describe temporal patterns in total community biomass among different groups (such as zooplankton or microalgae). This metric was calculated as temporal mean/temporal s.d. of the different trophic levels across the duration of the experiment. We calculated this stability measurement separately for zooplankton families (Fig. 3c) and microalgal phyla (Fig. 3f). Notably, stability often has many definitions[75]. In this study, high temporal stability would be indicated by a high value of this temporal stability metric, indicating biomass exhibited little change among groups and through time.

We checked models for meeting assumptions of homogeneity of variance and normality. For ANOVA and GAMM analyses, we considered treatment effects to be statistically significant based on $\alpha = 0.05$. For community trajectory analyses, we considered instances in which treatments exhibited non-overlapping 95% CIs to be statistically significantly different from one another. All statistical tests were performed in R (v.4.2.1).

Reporting summary

Further information on research design is available in the Nature Portfolio Reporting Summary linked to this article.

Data availability

All data for analyses are available at a permanent Zenodo repository (https://doi.org/10.5281/zenodo.10070514). Source data are provided with this paper.

Code availability

All code for analyses is available at a permanent Zenodo repository (https://doi.org/10.5281/zenodo.10070514).

40. Forbes, S. The lake as a microcosm. *INHS Bull.* **15**, 537–550 (1925).
41. Spivak, A. C., Vanni, M. J. & Mette, E. M. Moving on up: can results from simple aquatic mesocosm experiments be applied across broad spatial scales? *Freshw. Biol.* **56**, 279–291 (2011).
42. Dzialowski, A. R. et al. Are the abiotic and biotic characteristics of aquatic mesocosms representative of in situ conditions? *J. Limnol.* **73**, 603–612 (2014).
43. Bottrell, H. H. et al. A review of some problems in zooplankton production studies. *Nor. J. Zool.* **24**, 419–456 (1976).
44. Davis, C. S. & Wiebe, P. H. Macrozooplankton biomass in a warm-core Gulf Stream ring: time series changes in size structure, taxonomic composition, and vertical distribution. *J. Geophys. Res.* **90**, 8871–8884 (1985).
45. Menden-Deuer, S. & Lessard, E. J. Carbon to volume relationships for dinoflagellates, diatoms, and other protist plankton. *Limnol. Oceanogr.* **45**, 569–579 (2000).
46. Verity, P. G. et al. Relationships between cell volume and the carbon and nitrogen content of marine photosynthetic nanoplankton. *Limnol. Oceanogr.* **37**, 1434–1446 (1992).
47. Vanni, M. J. Competition in zooplankton communities: suppression of small species by *Daphnia pulex* 1: competition among zooplankton. *Limnol. Oceanogr.* **31**, 1039–1056 (1986).
48. Hall, D. J., Cooper, W. E. & Werner, E. E. An experimental approach to the production dynamics and structure of freshwater animal communities. *Limnol. Oceanogr.* **15**, 839–928 (1970).
49. Bartell, S. M. Influence of prey abundance on size-selective predation by bluegills. *Trans. Am. Fish. Soc.* **111**, 453–461 (1982).
50. Neiffer, D. L. & Stamper, M. A. Fish sedation, anesthesia, analgesia, and euthanasia: considerations, methods, and types of drugs. *ILAR J.* **50**, 343–360 (2009).
51. Barnett, A. J., Finlay, K. & Beisner, B. E. Functional diversity of crustacean zooplankton communities: towards a trait-based classification. *Freshw. Biol.* **52**, 796–813 (2007).
52. Cupertino, A., Gücker, B., Von Rückert, G. & Figueredo, C. C. Phytoplankton assemblage composition as an environmental indicator in routine lentic monitoring: taxonomic versus functional groups. *Ecol. Indic.* **101**, 522–532 (2019).
53. Arar, E. J. *In Vitro Determination of Chlorophyll* a *and Pheophytin* a *in Marine and Freshwater Algae by Fluorescence*.(Environmental Protection Agency, 1997).
54. *Standard Operating Procedure For In Vitro Determination of Chlorophyll-a in Freshwater Phytoplankton by Fluorescence* (Environmental Protection Agency, 2013).
55. Knefelkamp, B., Carstens, K. & Wiltshire, K. H. Comparison of different filter types on chlorophyll-*a* retention and nutrient measurements. *J. Exp. Mar. Biol. Ecol.* **345**, 61–70 (2007).
56. Arar, E. J. *Evaluation of a New Fluorometric Technique That Uses Highly Selective Interference Filters For Measuring Chlorophyll* a *in the Presence of Chlorophyll* b *and Pheopigments* (Environmental Protection Agency, 1994).
57. Welschmeyer, N. A. Fluorometric analysis of chlorophyll *a* in the presence of chlorophyll *b* and pheopigments. *Limnol. Oceanogr.* **39**, 1985–1992 (1994).
58. Hrycik, A. R., Shambaugh, A. & Stockwell, J. D. Comparison of FlowCAM and microscope biovolume measurements for a diverse freshwater phytoplankton community. *J. Plankton Res.* **41**, 849–864 (2019).
59. Breier, C. F. & Buskey, E. J. Effects of the red tide dinoflagellate, *Karenia brevis*, on grazing and fecundity in the copepod *Acartia tonsa*. *J. Plankton Res.* **29**, 115–126 (2007).
60. Mack, H. R., Conroy, J. D., Blocksom, K. A., Stein, R. A. & Ludsin, S. A. A comparative analysis of zooplankton field collection and sample enumeration methods: zooplankton sampling and counting methods. *Limnol. Oceanogr. Methods* **10**, 41–53 (2012).
61. Bogdan, K. G. & Gilbert, J. J. Body size and food size in freshwater zooplankton. *Proc. Natl Acad. Sci. USA* **81**, 6427–6431 (1984).
62. Brown, J. H., Gillooly, J. F., Allen, A. P., Savage, V. M. & West, G. B. Toward a metabolic theory of ecology. *Ecology* **85**, 1771–1789 (2004).
63. Peters, R. H. *The Ecological Implications of Body Size* (Cambridge Univ. Press, 1983).
64. Savage, V. M., Gillooly, J. F., Brown, J. H., West, G. B. & Charnov, E. L. Effects of body size and temperature on population growth. *Am. Nat.* **163**, 429–441 (2004).
65. De Gooijer, J. G. & Hyndman, R. J. 25 years of time series forecasting. *Int. J. Forecast.* **22**, 443–473 (2006).
66. Robert, H. S. & Stoffer, D. S. *Time Series Analysis and Its Application* (Springer, 2017).
67. De Livera, A. M., Hyndman, R. J. & Snyder, R. D. Forecasting time series with complex seasonal patterns using exponential smoothing. *J. Am. Stat. Assoc.* **106**, 1513–1527 (2011).
68. Mann, M. E. Smoothing of climate time series revisited. *Geophys. Res. Lett.* **35**, L16708 (2008).
69. Wood, S. N. Stable and efficient multiple smoothing parameter estimation for generalized additive models. *J. Am. Stat. Assoc.* **99**, 673–686 (2004).
70. Pinherio, J., Bates, D. & R Core Team. nlme: linear and nonlinear mixed effects models (2022).
71. Wood, S. N. Thin-plate regression spine. *J. R. Stat. Soc. B* **65**, 95–114 (2003).
72. Sturbois, A. et al. Extending community trajectory analysis: new metrics and representation. *Ecol. Modell.* **440**, 109400 (2021).
73. Dexter, E., Rollwagen-Bollens, G. & Bollens, S. M. The trouble with stress: a flexible method for the evaluation of nonmetric multidimensional scaling. *Limnol. Oceanogr. Methods* **16**, 434–443 (2018).
74. Tilman, D. The ecological consequences of changes in biodiversity: a search for general principles. *Ecology* **80**, 1455–1474 (1999).
75. Domínguez-García, V., Dakos, V. & Kéfi, S. Unveiling dimensions of stability in complex ecological networks. *Proc. Natl Acad. Sci. USA* **116**, 25714–25720 (2019).

Author contributions S.P.T., S.B.F., J.P.G. and A.M.S. developed the idea and experimental approach. A.M.S. secured funding and supervised the project. S.P.T. conducted the experiment, compiled data and conducted analyses. S.P.T., S.B.F., J.P.G. and A.M.S. wrote the manuscript and contributed to revisions.
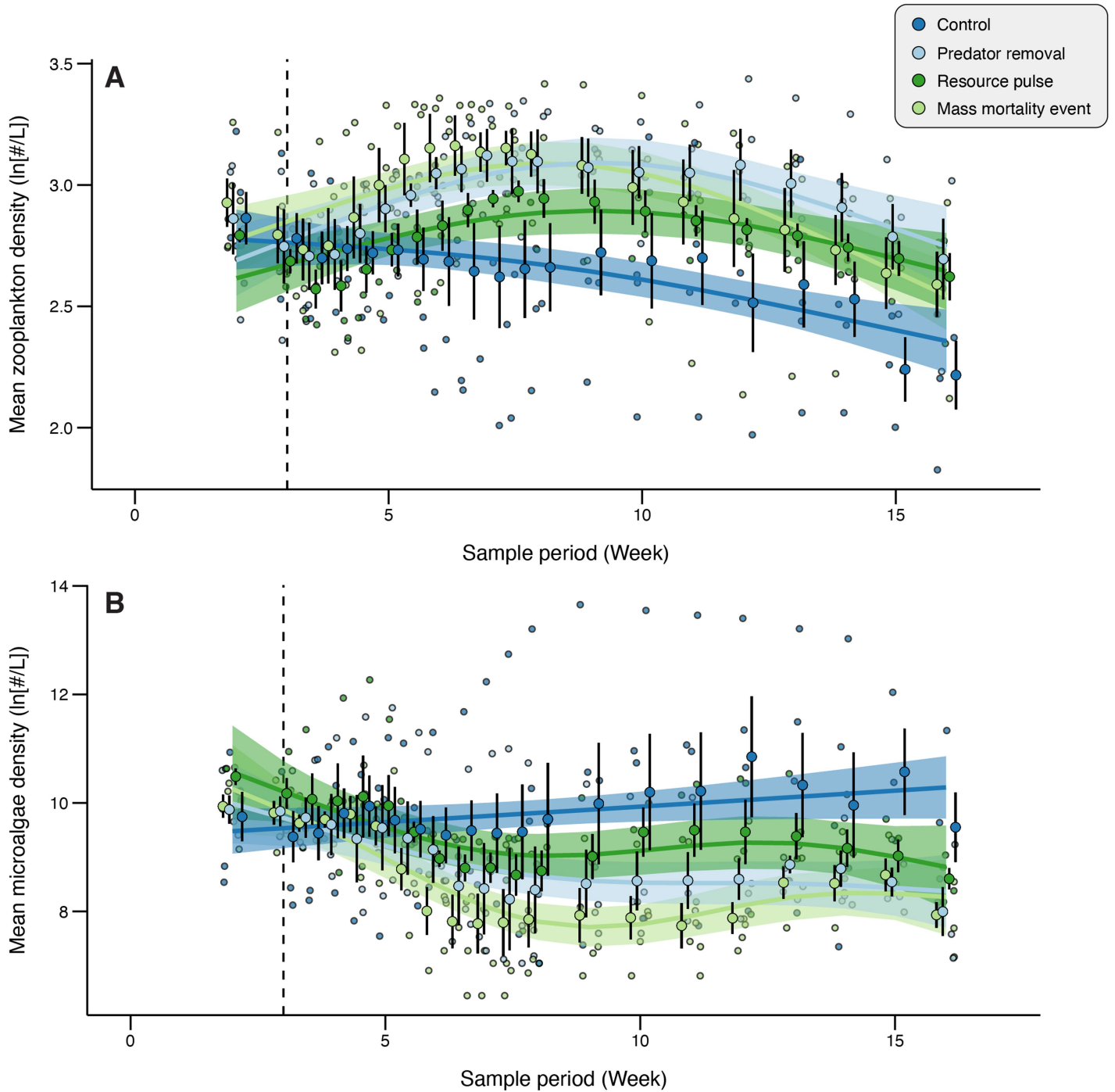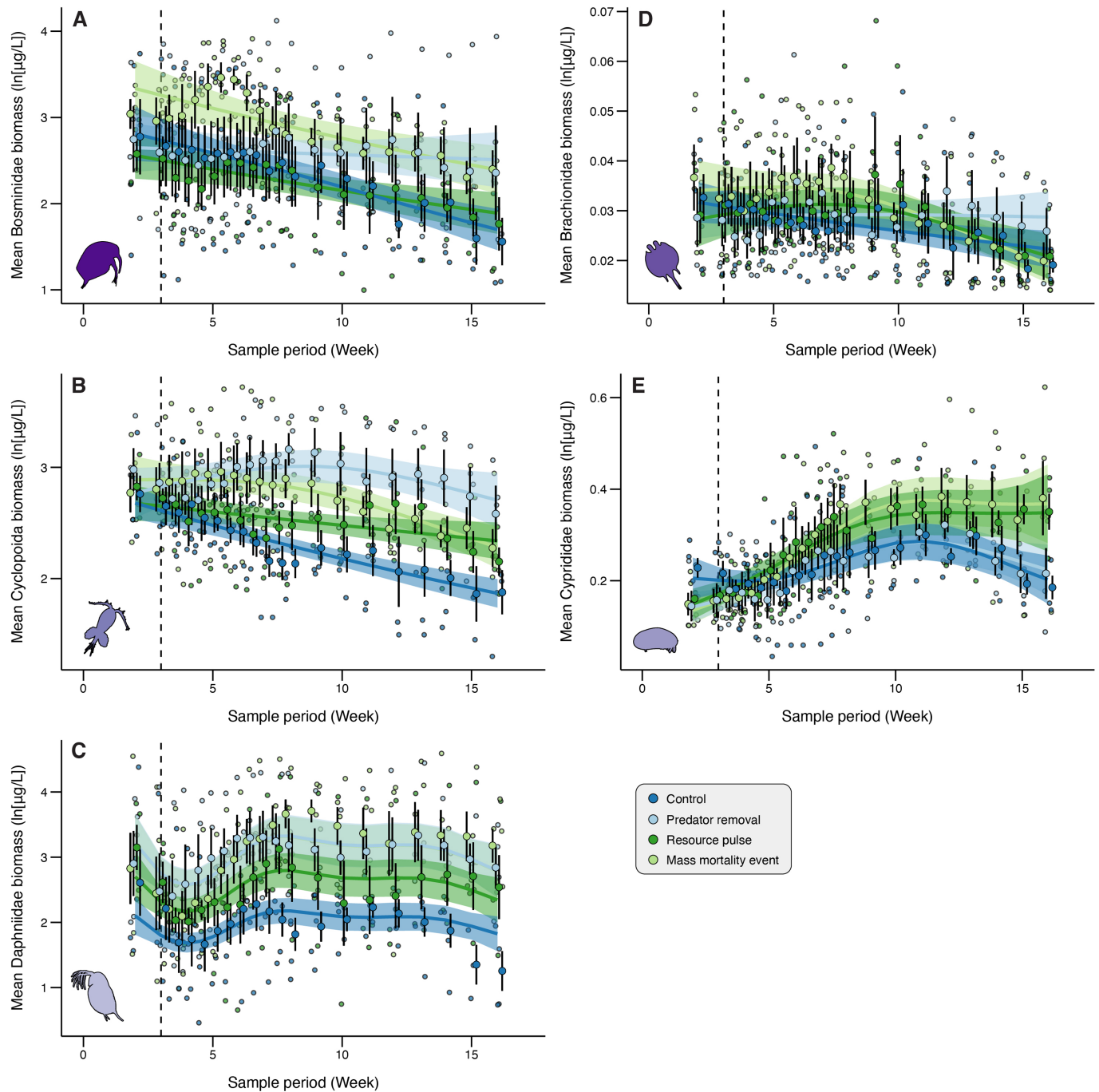
Extended Data Fig. 1 | Time series of mean zooplankton and microalgae density following ecological perturbations. Mean density (ln[individuals/L]) of zooplankton (A) and microalgae (B) following predator mass mortality events (MMEs, light green), predator removals (light blue), and resource pulses (dark green), as well as the undisturbed system (control, dark blue). Points and lines indicate mean values and +/−1 SE for each sampling period and treatment, with points jittered to reduce overlap within sample periods. Solid lines and shaded regions indicate model predictions and 95% confidence intervals, respectively. Relative to the control, MMEs ($t_{11.42} = 7.51$, $p < 0.01$), predator removals ($t_{11.42} = 7.35$, $p < 0.01$), and, to a lesser extent, resource pulses ($t_{11.42} = 3.73$, $p < 0.01$) increased mean zooplankton density. MMEs ($t_{13.36} = −7.95$, $p < 0.01$), predator removals ($t_{13.36} = −5.28$, $p < 0.01$), and, to a lesser extent, resource pulses ($t_{13.36} = −2.43$, $p = 0.02$) decreased mean microalgae density. Dashed lines indicate when perturbations were induced (i.e., live fish and/or fish carrion added and/or removed). Data were analysed from 355 biologically independent zooplankton samples (A) and microalgae samples (B) for a control ($n = 96$), predator removal ($n = 80$), resource pulse ($n = 80$), and MME ($n = 99$), respectively, from one experiment. General additive mixed model (GAMM, A-B).
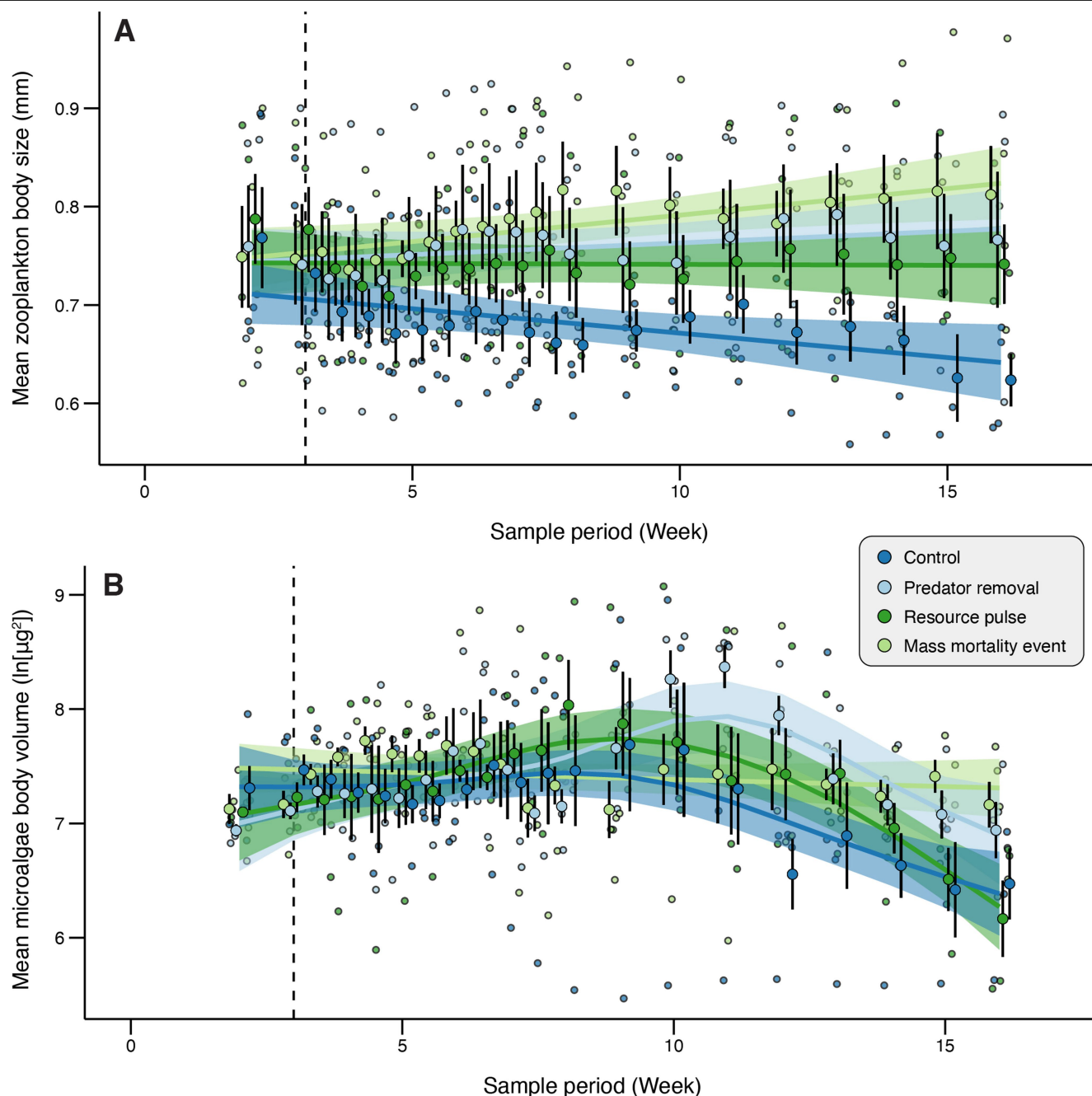
Extended Data Fig. 2 | Time series of mean zooplankton body size and microalgae biovolume following ecological perturbations. Mean zooplankton body size (mm, A) and microalgae biovolume (ln[μm²], B) following predator mass mortality events (MMEs, light green), predator removals (light blue), and resource pulses (dark green), as well as the undisturbed system (control, dark blue). Points and lines indicate mean values and +/− 1 SE for each sampling period and treatment, with points jittered to reduce overlap within sample periods. Solid lines and shaded regions indicate model predictions and 95% confidence intervals, respectively. Relative to the control, MMEs ($t_8 = 8.42$,

$p < 0.01$), predator removals ($t_8 = 6.29$, $p < 0.01$), and resource pulses ($t_8 = 4.99$, $p < 0.01$) increased mean zooplankton body size. MMEs ($t_{15.06} = 2.58$, $p = 0.02$) and predator removals ($t_{15.06} = 2.48$, $p = 0.02$), but not resource pulses ($t_{15.06} = 1.32$, $p = 0.19$), increased mean microalgae biovolume. Dashed lines indicate when perturbations were induced (i.e., live fish and/or fish carrion added and/or removed). Data were analysed from 355 biologically independent zooplankton samples (A) and microalgae samples (B) for a control ($n = 96$), predator removal ($n = 80$), resource pulse ($n = 80$), and MME ($n = 99$), respectively, from one experiment. General additive mixed model (GAMM, A-B).

Extended Data Fig. 3 | Time series of mean biomass across five major zooplankton families following ecological perturbations. Zooplankton biomass (ln[µg/L]) of Bosminidae (A), Brachionidae (B), Cyclopoida (C), Cyprididae (D), and Daphniidae (E) following predator mass mortality events (MMEs, light green), predator removals (light blue), and resource pulses (dark green), as well the undisturbed system (control, dark blue). Points and lines indicate mean values and +/−1 SE for each sampling period and treatment, with points jittered to reduce overlap within sample periods. Solid lines and shaded regions indicate model predictions and 95% confidence intervals, respectively. Relative to the control, MMEs increased mean biomass of Bosminidae ($t_{8.36} = 5.74$, $p < 0.01$; A), Brachionidae ($t_{9.78} = 2.31$, $p = 0.02$; B), Cyclopoida ($t_{9.59} = 8.33$, $p < 0.01$; C), Cyprididae ($t_{15} = 2.98$, $p < 0.01$; D), and Daphniidae ($t_{9.34} = 9.31$, $p < 0.01$; E).

Predator removals increased mean biomass of Bosminidae ($t_{8.36} = 2.70$, $p = 0.008$; A), Cyclopoida ($t_{9.59} = 10.49$, $p < 0.01$; C) and Daphniidae ($t_{9.34} = 8.84$, $p < 0.01$; E). Resource pulses increased mean biomass of Cyclopoida ($t_{9.59} = 8.42$, $p < 0.01$; C), Cyprididae ($t_{15} = 2.30$, $p = 0.01$; D), and Daphniidae ($t_{9.34} = 5.23$, $p < 0.01$; E). Dashed lines indicate when perturbations were induced (i.e., live fish and/or fish carrion added and/or removed). Taxa silhouettes and their colours correspond with major zooplankton families as in main figures. Data were analysed from 355 biologically independent zooplankton samples (A-E) for a control ($n = 96$), predator removal ($n = 80$), resource pulse ($n = 80$), and MME ($n = 99$), respectively, from one experiment. General additive mixed model (GAMM, A-E).
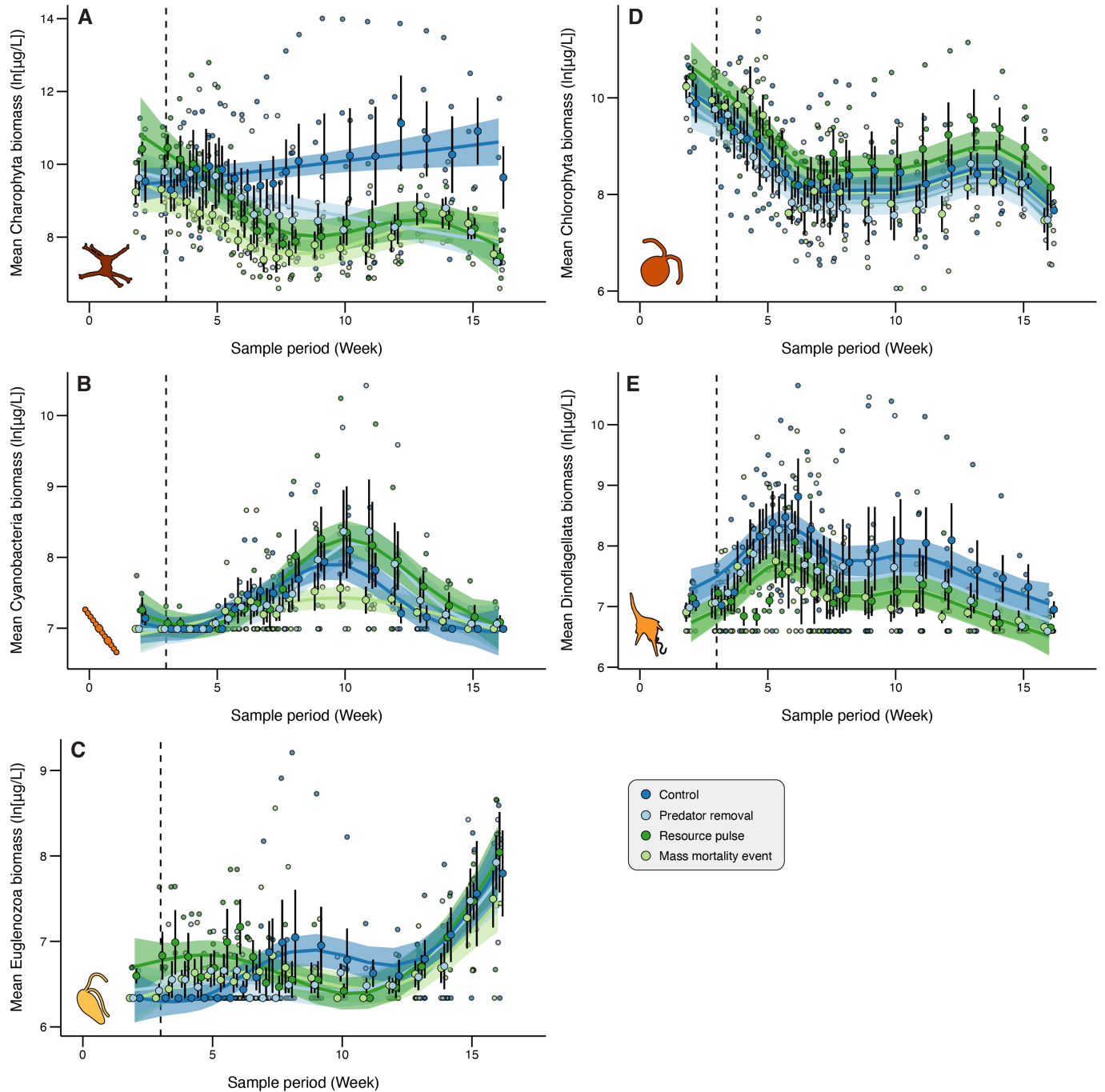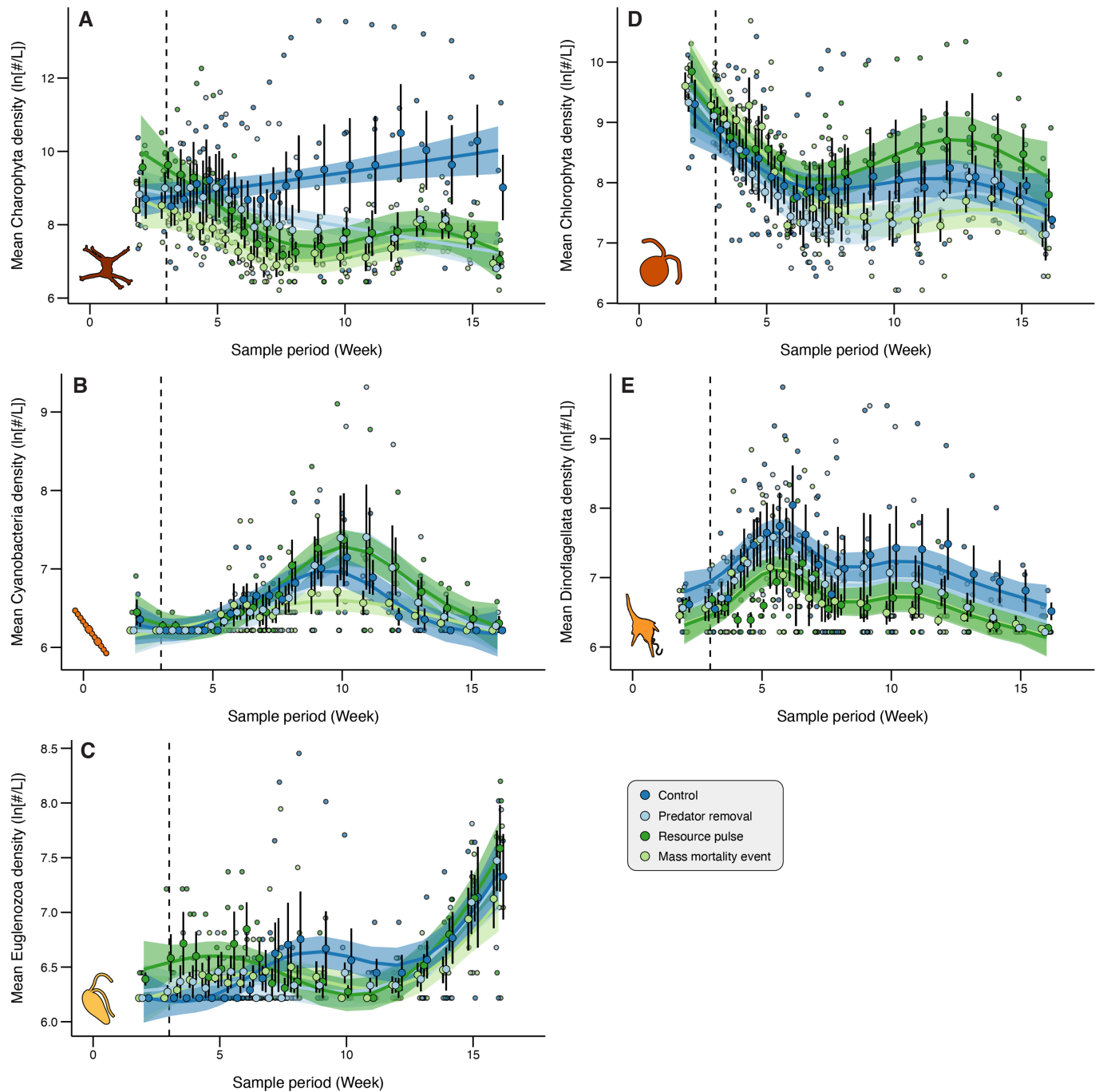
Extended Data Fig. 4 | Time series of mean biomass across five major microalgae phyla following ecological perturbations. Microalgae biomass (ln[µg/L]) of Charophyta (A), Chlorophyta (B), Cyanobacteria (C), Dinoflagellata (D), and Euglenozoa (E) following predator mass mortality events (MMEs, light green), predator removals (light blue), and resource pulses (dark green), as well the undisturbed system (control, dark blue). Points and lines indicate mean values and +/− 1 SE for each sampling period and treatment, with points jittered to reduce overlap within sample periods. Solid lines and shaded regions indicate model predictions and 95% confidence intervals, respectively. Relative to the control, MMEs decreased mean biomass of Charophyta ($t_{12.81} = -9.93$, $p < 0.01$; A) and Dinoflagellata ($t_{22.1} = -5.04$, $p < 0.01$; D), and had relatively low mean Cyanobacteria biomass ($t_{22.1} = -1.85$, $p = 0.07$; C).

Predator removals decreased mean biomass of Charophyta ($t_{12.81} = -5.69$, $p < 0.01$; A) and Dinoflagellata ($t_{22.1} = -2.47$, $p = 0.01$; D). Resource pulses increased mean biomass of Chlorophyta ($t_{10.01} = 3.19$, $p = 0.01$; B) and Cyanobacteria ($t_{22.1} = 2.05$, $p = 0.04$; C), and decreased mean biomass of Charophyta ($t_{12.81} = -6.07$, $p < 0.01$; A) and Dinoflagellata ($t_{22.1} = -4.89$, $p < 0.01$; D). Dashed lines indicate when perturbations were induced (i.e., live fish and/or fish carrion added and/or removed). Taxa silhouettes and their colours correspond with major microalgae phyla as in main figures. Data were analysed from 355 biologically independent zooplankton samples (A-E) for a control ($n = 96$), predator removal ($n = 80$), resource pulse ($n = 80$), and MME ($n = 99$), respectively, from one experiment. General additive mixed model (GAMM, A-E).
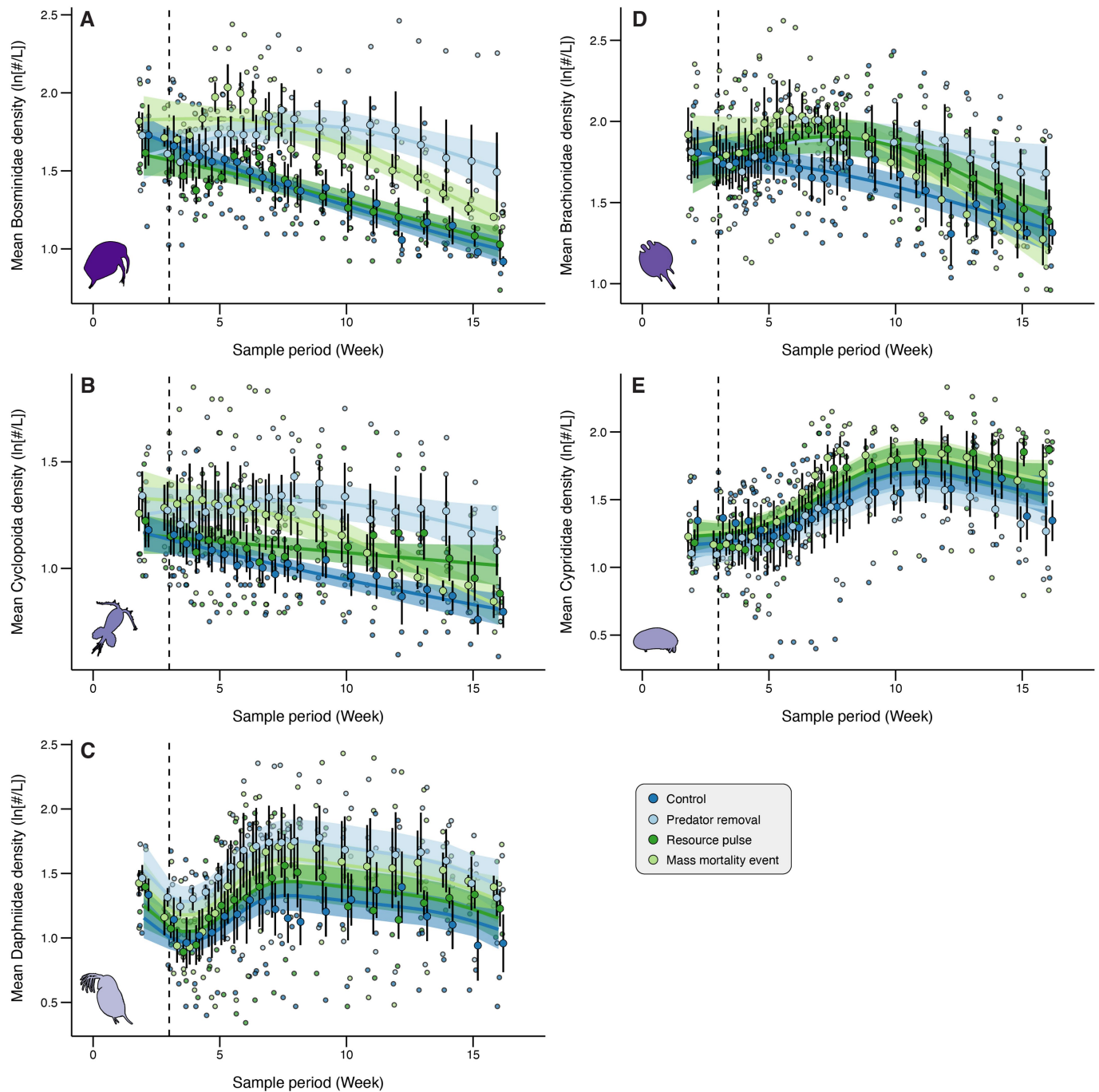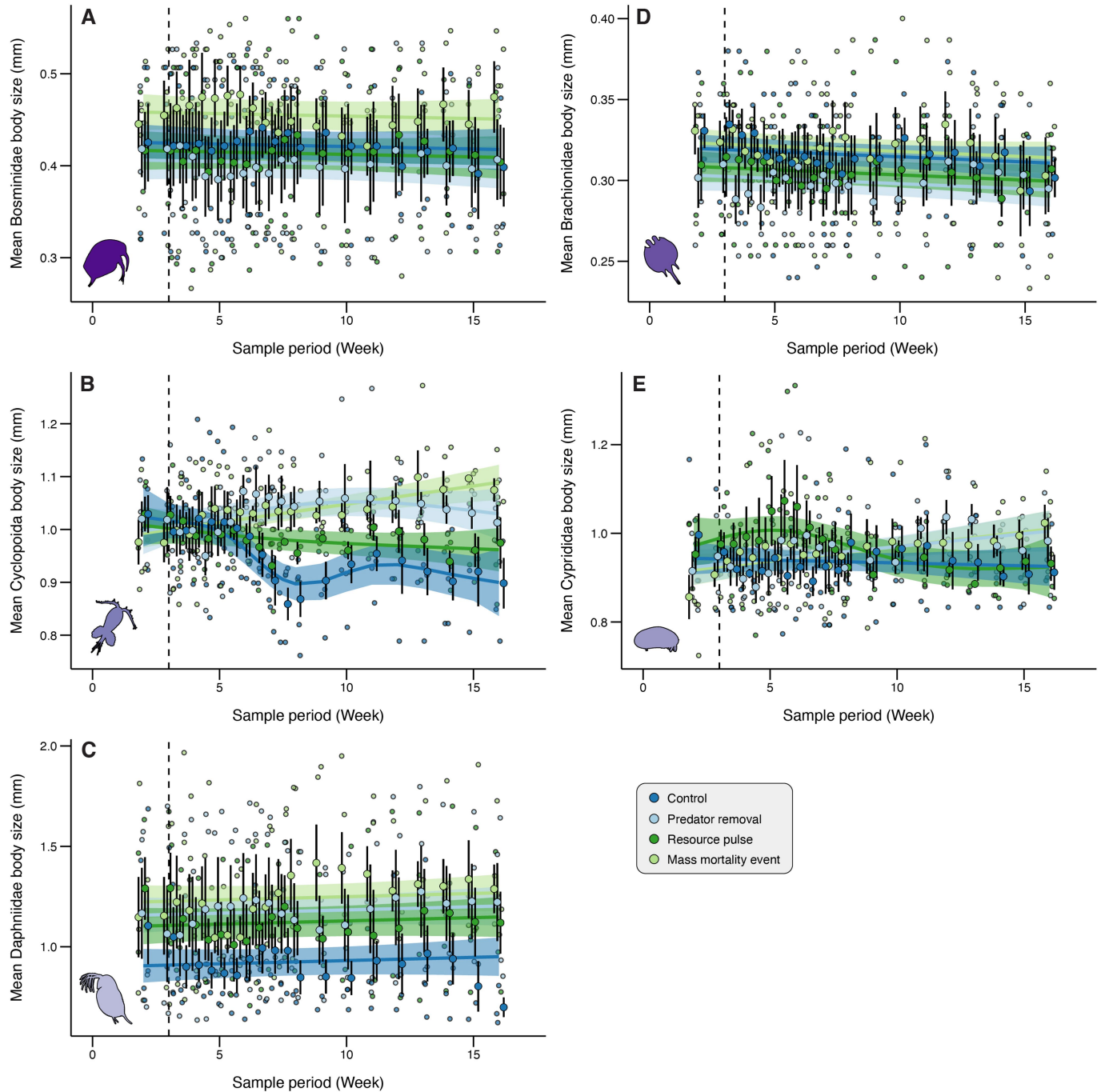
Extended Data Fig. 5 | Time series of mean density across five major zooplankton families following ecological perturbations. Zooplankton density (ln[individuals/L]) of Bosminidae (A), Brachionidae (B), Cyclopoida (C), Cyprididae (D), and Daphniidae (E) following predator mass mortality events (MMEs, light green), predator removals (light blue), and resource pulses (dark green), as well as the undisturbed system (control, dark blue). Points and lines indicate mean values and +/−1 SE for each sampling period and treatment, with points jittered to reduce overlap within sample periods. Solid lines and shaded regions indicate model predictions and 95% confidence intervals, respectively. Relative to the control, MMEs increased mean density of all major zooplankton families including Bosminidae ($t_{10.4} = 8.05, p < 0.01$; A), Brachionidae ($t_{11.13} = 3.00$, $p < 0.01$; B), Cyclopoida ($t_{9.53} = 5.70, p < 0.01$; C), Cyprididae ($t_{7.44} = 2.09$,

$p = 0.04$; D), and Daphniidae ($t_{9.4} = 4.38, p < 0.01$; E). Predator removals increased mean density of Bosminidae ($t_{10.4} = 8.36, p < 0.01$; A), Brachionidae ($t_{11.13} = 4.12, p < 0.01$; B), Cyclopoida ($t_{9.53} = 8.34, p < 0.01$; C), and Daphniidae ($t_{9.4} = 5.95, p < 0.01$; E) as well as reduced mean Cyprididae density ($t_{7.44} = -1.98$, $p = 0.05$; D). Resource pulses increased mean density of Brachionidae ($t_{11.13} = 2.99$, $p < 0.01$; B) and Cyclopoida ($t_{9.53} = 3.13, p < 0.01$; C). Dashed lines indicate when perturbations were induced (i.e., live fish and/or fish carrion added and/or removed). Taxa silhouettes and their colours correspond with major zooplankton families as in main figures. Data were analysed from 355 biologically independent zooplankton samples (A-E) for a control ($n = 96$), predator removal ($n = 80$), resource pulse ($n = 80$), and MME ($n = 99$), respectively, from one experiment. General additive mixed model (GAMM, A-E).

Extended Data Fig. 6 | Time series of mean density across five major microalgae phyla following ecological perturbations. Microalgae density (ln([ndividuals/L]) of Charophyta (A), Chlorophyta (B), Cyanobacteria (C), Dinoflagellata (D), and Euglenozoa (E) following predator mass mortality events (MMEs, light green), predator removals (light blue), and resource pulses (dark green), as well as the undisturbed system (control, dark blue). Points and lines indicate mean values and +/− 1 SE for each sampling period and treatment, with points jittered to reduce overlap within sample periods. Solid lines and shaded regions indicate model predictions and 95% confidence intervals, respectively. Relative to the control, MMEs decreased mean density of Charophyta ($t_{12.42} = -9.83$, $p < 0.01$; A) and Dinoflagellata ($t_{9.87} = -5.18$, $p < 0.01$; D), as well as had relatively low mean density of Cyanobacteria ($t_{21.86} = -1.67$, $p = 0.10$; C).

Predator removals decreased density of Charophyta ($t_{12.42} = -5.63$, $p < 0.01$; A), Chlorophyta ($t_{17.14} = -2.47$, $p = 0.02$; B), and Dinoflagellata ($t_{9.87} = -5.18$, $p < 0.01$; D). Resource pulses increased mean density of Chlorophyta ($t_{17.14} = 2.86$, $p = 0.01$; B) and reduced mean density of Charophyta ($t_{12.42} = -5.98$, $p < 0.01$; A) and Dinoflagellata ($t_{9.87} = -5.11$, $p < 0.01$; D), as well as had relatively high mean density of Cyanobacteria ($t_{21.86} = 1.93$, $p = 0.06$; C). Dashed lines indicate when perturbations were induced (i.e., live fish and/or fish carrion added and/or removed). Taxa silhouettes and their colours correspond with major microalgae phyla as in main figures. Data were analysed from 355 biologically independent zooplankton samples (A-E) for a control ($n = 96$), predator removal ($n = 80$), resource pulse ($n = 80$), and MME ($n = 99$), respectively, from one experiment. General additive mixed model (GAMM, A-E).
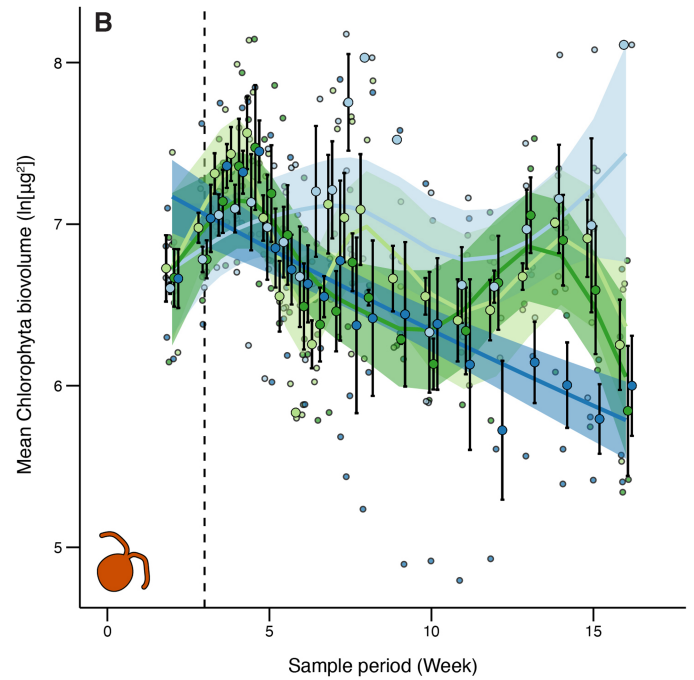
Extended Data Fig. 7 | Time series of mean body size across five major zooplankton families following ecological perturbations. Zooplankton body size (mm) of Bosminidae (A), Brachionidae (B), Cyclopoida (C), Cyprididae (D), and Daphniidae (E) following predator mass mortality events (MMEs, light green), predator removals (light blue), and resource pulses (dark green), as well as the undisturbed system (control, dark blue). Points and lines indicate mean values and +/−1 SE for each sampling period and treatment, with points jittered to reduce overlap within sample periods. Solid lines and shaded regions indicate model predictions and 95% confidence intervals, respectively. Relative to the control, MMEs increased mean body size of Bosminidae ($t_5 = 2.98, p < 0.01$; A), Cyclopoida ($t_{12.93} = 7.57, p < 0.01$; C), and Daphniidae ($t_5 = 6.71, p < 0.01$; E). Predator removals increased mean body size of Cyclopoida ($t_{12.93} = 6.98, p < 0.01$; C) and

Daphniidae ($t_5 = 5.09, p < 0.001$; E), as well as decreased mean body size of Brachionidae ($t_5 = -3.17, p < 0.01$; B). Resource pulses increased mean body size of Cyclopoida ($t_{12.93} = 2.68, p = 0.01$; C), Cyprididae ($t_{9.74} = 2.16, p = 0.03$; D), and Daphniidae ($t_5 = 3.88, p < 0.01$; E), as well as decreased mean body size of Brachionidae ($t_5 = -2.14, p = 0.03$; B). Dashed lines indicate when perturbations were induced (i.e., live fish and/or fish carrion added and/or removed). Taxa silhouettes and their colours correspond with major zooplankton families as in main figures. Data were analysed from 355 biologically independent zooplankton samples (A-E) for a control ($n = 96$), predator removal ($n = 80$), resource pulse ($n = 80$), and MME ($n = 969$, respectively, from one experiment. General additive mixed model (GAMM, A-E).
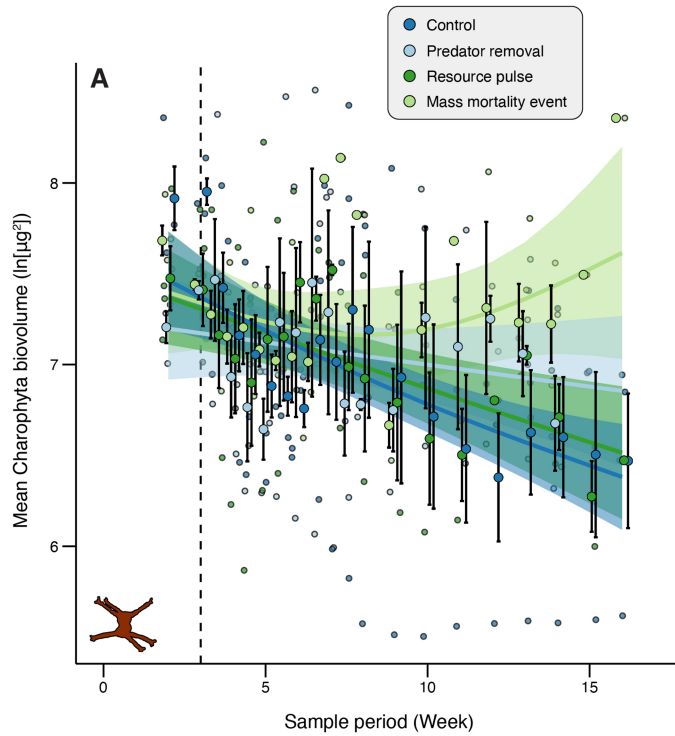
Extended Data Fig. 8 | Time series of mean biovolume across two major microalgae phyla following ecological perturbations. Mean microalgae biovolume (ln[μg²]) of Charophyta (A) and Chlorophyta (B) following predator mass mortality events (MMEs, light green), predator removals (light blue), and resource pulses (dark green), as well as the undisturbed system (control, dark blue). Points and lines indicate mean values and +/− 1 SE for each sampling period and treatment, with points jittered to reduce overlap within sample periods. Solid lines and shaded regions indicate model predictions and 95% confidence intervals, respectively. Relative to the control, MMEs increased mean biovolume of Charophyta ($t_{8.83}$ = 2.47, p = 0.01; A) and Chlorophyta ($t_{20.96}$ = 2.93, p < 0.01; B). Predator removals increased mean biovolume of Chlorophyta ($t_{20.96}$ = 4.32, p < 0.01; A). Dashed lines indicate when perturbations were induced (i.e., live fish and/or fish carrion added and/or removed). Taxa silhouettes and their colours correspond with major microalgae phyla as in main figures. Data were analysed from 240 biologically independent samples of Charophyta (A) for a control, (n = 80), predator removal (n = 54), resource pulse (n = 54), and MME (n = 52), as well as 283 biologically independent samples of Chlorophyta (B) for a control, (n = 79), predator removal (n = 59), resource pulse (n = 70), and MME (n = 75), from one experiment. General additive mixed model (GAMM, A-B).
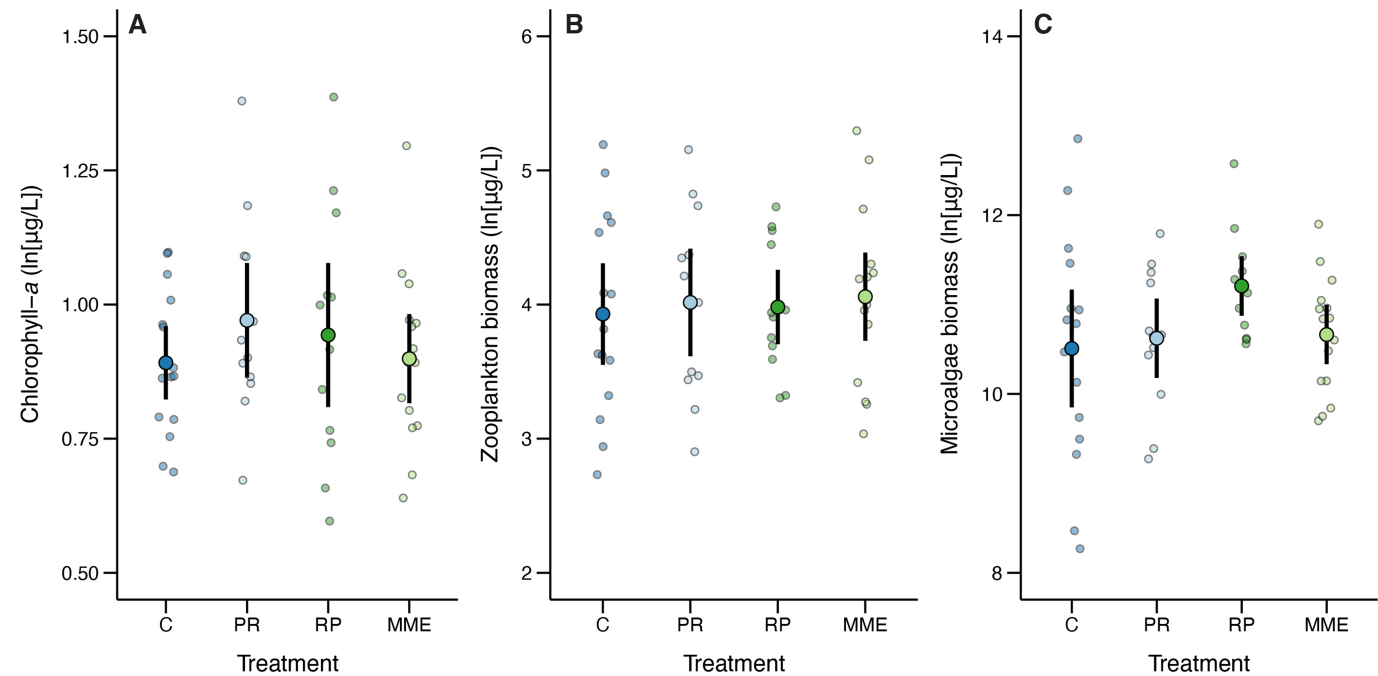
Extended Data Fig. 9 | Raw biomass estimates during sample periods before ecological perturbations were induced (i.e., the first three sample periods). Chlorophyll-*a* (ln[µg/L], A), zooplankton biomass (ln[µg/L], B), and microalgae biomass (ln[µg/L], C) in mesocosms that would receive treatments to become predator mass mortality events (MMEs, light green), predator removals (light blue), and resource pulses (dark green), as well as the undisturbed system (control, dark blue). Large points and lines indicate mean values and 95% CIs, with smaller jittered points (to reduce overlap) indicating individual samples. There were no effects of treatment on average chlorophyll-*a* ($F_{1,3} = 0.11$, $p = 0.65$; A), zooplankton biomass ($F_{1,3} = 0.03$, $p = 0.99$; B), or microalgae biomass ($F_{1,3} = 0.94$, $p = 0.45$; C) during the first three sample periods of the experiment. Data were analysed from 54 biologically independent samples for a control, ($n = 15$), predator removal ($n = 12$), resource pulse ($n = 12$), and MME ($n = 15$). Two-way, two-sided ANOVA (A-B).
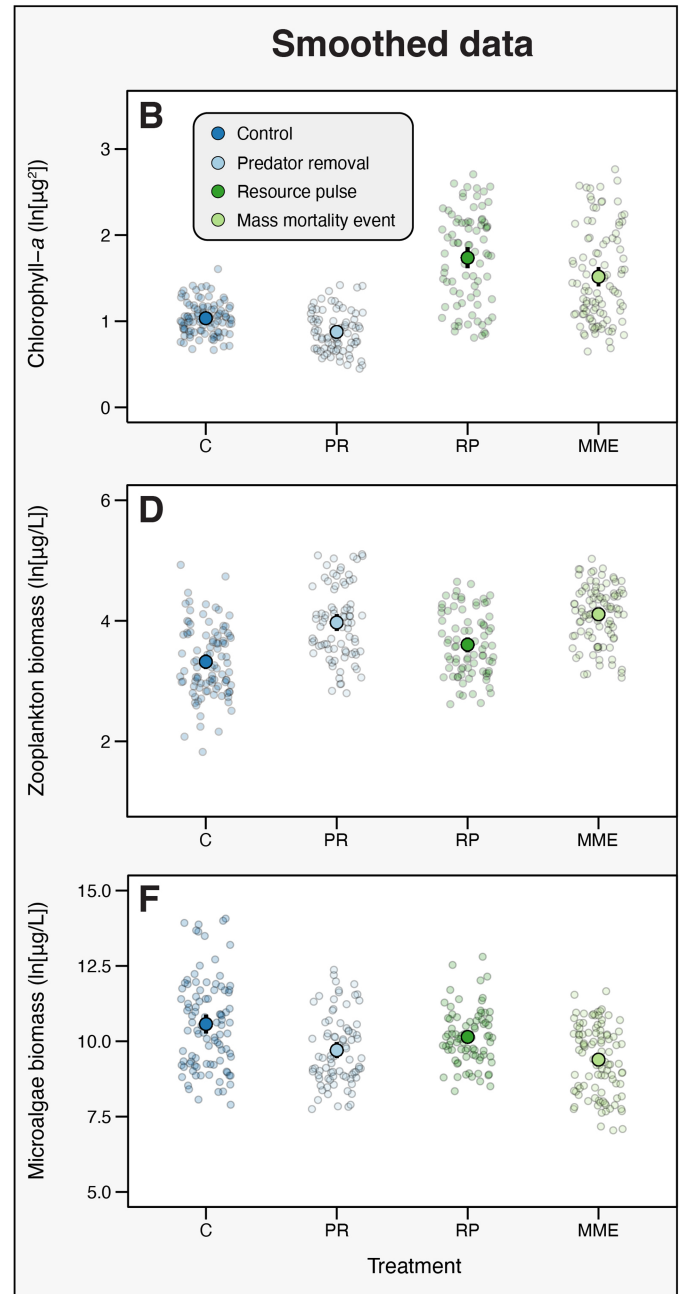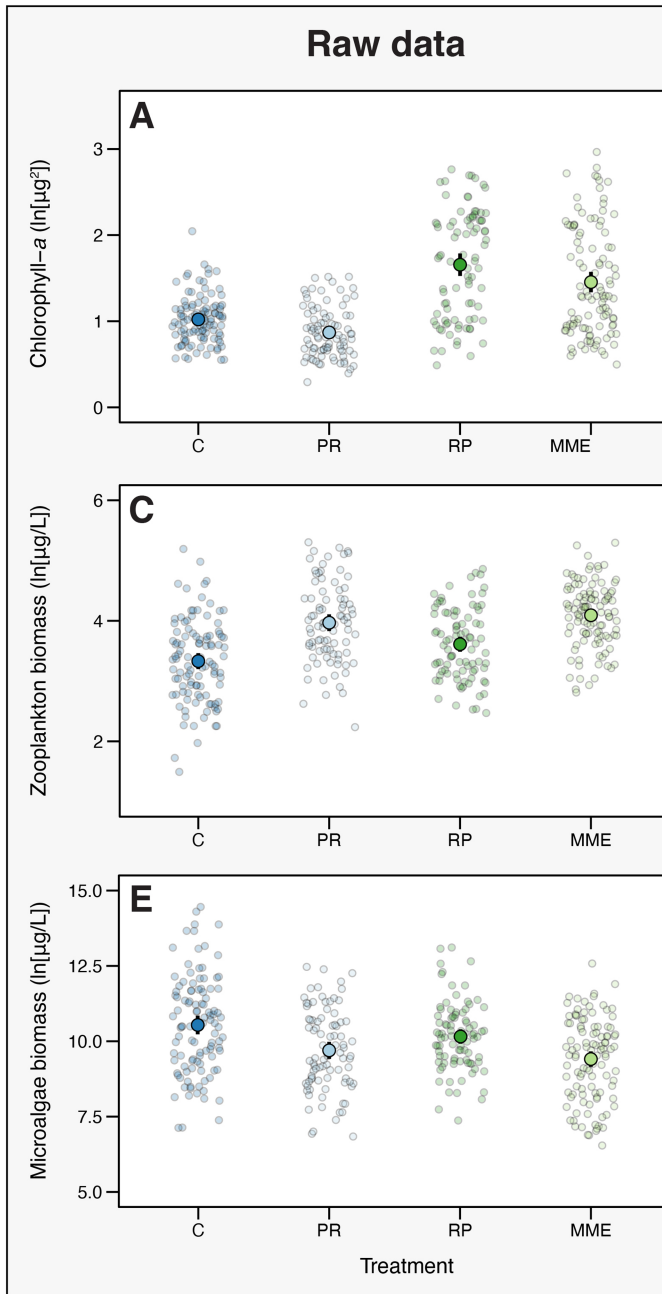
Extended Data Fig. 10 | Raw (non-smoothed) and smoothed biomass estimates following ecological perturbations. Chlorophyll-*a* (ln[µg/L], A-B), zooplankton biomass (ln[µg/L], C-D), and microalgae biomass (ln[µg/L], E-F) following predator mass mortality events (MMEs, light green), predator removals (light blue), and resource pulses (dark green), as well as the undisturbed system (control, dark blue). Points and lines indicate mean values and 95% CIs, with points jittered to reduce overlap. Raw data (A, C, E) were similar to smoothed data (B, D, F, as in Fig. 1f–h). Specifically, relative to the experimental control, predator removals decreased average chlorophyll-*a* ($F_{1,14} = 5.50$, $p = 0.03$; A), resource pulses increased average chlorophyll-*a* ($F_{1,14} = 151.48$, $p < 0.01$), and there was no significant interaction between predator removals and resource pulses (i.e., MMEs) on chlorophyll-*a* ($F_{1,14} = 0.26$, $p = 0.62$). Additionally, predator removals increased zooplankton biomass ($F_{1,14} = 5.03$, $p = 0.04$; C), but there

was no effect of resource pulses on zooplankton biomass ($F_{1,14} = 0.56$, $p = 0.47$) nor was there a significant interaction between predator removals and resource pulses on zooplankton biomass ($F_{1,14} = 0.07$, $p = 0.80$). Lastly, there was strong evidence that predator removals reduced microalgae biomass ($F_{1,14} = 4.16$, $p = 0.06$; E), but there was no effect of resource pulses on microalgae biomass ($F_{1,14} = 0.64$, $p = 0.43$) nor was there a significant interaction between predator removals and resource pulses on microalgae biomass ($F_{1,14} = 0.01$, $p = 0.94$). Results for the analysis of the smoothed data are shown in the main text. Raw data were analysed from 391 biologically independent samples for a control ($n = 106$), predator removal ($n = 88$), resource pulse ($n = 88$), and MME ($n = 109$). Smoothed data were analysed from 355 biologically independent samples for a control ($n = 96$), predator removal ($n = 80$), resource pulse ($n = 80$), and MME ($n = 99$), from one experiment. Two-way, two-sided ANOVA (A-B).

nature portfolio

Corresponding author(s): Simon P. Tye

Last updated by author(s): Nov 3, 2023

Reporting Summary

Nature Portfolio wishes to improve the reproducibility of the work that we publish. This form provides structure for consistency and transparency in reporting. For further information on Nature Portfolio policies, see our [Editorial Policies](#) and the [Editorial Policy Checklist](#).

Statistics

For all statistical analyses, confirm that the following items are present in the figure legend, table legend, main text, or Methods section.

n/a	Confirmed	
☐	☒	The exact sample size (n) for each experimental group/condition, given as a discrete number and unit of measurement
☐	☒	A statement on whether measurements were taken from distinct samples or whether the same sample was measured repeatedly
☐	☒	The statistical test(s) used AND whether they are one- or two-sided *Only common tests should be described solely by name; describe more complex techniques in the Methods section.*
☐	☒	A description of all covariates tested
☐	☒	A description of any assumptions or corrections, such as tests of normality and adjustment for multiple comparisons
☐	☒	A full description of the statistical parameters including central tendency (e.g. means) or other basic estimates (e.g. regression coefficient) AND variation (e.g. standard deviation) or associated estimates of uncertainty (e.g. confidence intervals)
☐	☒	For null hypothesis testing, the test statistic (e.g. F, t, r) with confidence intervals, effect sizes, degrees of freedom and P value noted *Give P values as exact values whenever suitable.*
☒	☐	For Bayesian analysis, information on the choice of priors and Markov chain Monte Carlo settings
☒	☐	For hierarchical and complex designs, identification of the appropriate level for tests and full reporting of outcomes
☒	☐	Estimates of effect sizes (e.g. Cohen's d, Pearson's r), indicating how they were calculated

Our web collection on [statistics for biologists](#) contains articles on many of the points above.

Software and code

Policy information about [availability of computer code](#)

Data collection	We used custom code that is available on a Zenodo repository (doi:10.5281/zenodo.10070579).
Data analysis	We used R (version 4.2.1) for all analyses. Statistical analyses required several R packages, including nlme (Version 3.1-157), mgcv (Version 1.8-40), and ecotraj (Version 0.0.3). All other packages that were used are listed at the top of each script within the Zenodo repository.

For manuscripts utilizing custom algorithms or software that are central to the research but not yet described in published literature, software must be made available to editors and reviewers. We strongly encourage code deposition in a community repository (e.g. GitHub). See the Nature Portfolio [guidelines for submitting code & software](#) for further information.

Data

Policy information about [availability of data](#)

All manuscripts must include a [data availability statement](#). This statement should provide the following information, where applicable:
- Accession codes, unique identifiers, or web links for publicly available datasets
- A description of any restrictions on data availability
- For clinical datasets or third party data, please ensure that the statement adheres to our [policy](#)

All data for analyses are available on a Zenodo repository (doi:10.5281/zenodo.10070579).

Human research participants

Policy information about [studies involving human research participants and Sex and Gender in Research.](#)

Reporting on sex and gender	NA
Population characteristics	NA
Recruitment	NA
Ethics oversight	NA

Note that full information on the approval of the study protocol must also be provided in the manuscript.

Field-specific reporting

Please select the one below that is the best fit for your research. If you are not sure, read the appropriate sections before making your selection.

☐ Life sciences ☐ Behavioural & social sciences ☒ Ecological, evolutionary & environmental sciences

For a reference copy of the document with all sections, see [nature.com/documents/nr-reporting-summary-flat.pdf](#)

Ecological, evolutionary & environmental sciences study design

All studies must disclose on these points even when the disclosure is negative.

Study description	We aimed to examine whether ecological dynamics following predator mass mortality events (MMEs, top-down and bottom-up effect) were distinct from similar ecological perturbations: predator removals (only top-down effect) and resource pulses (only bottom-up effect) We focused these inquiries on freshwater food webs. We therefore constructed 20 freshwater mesocosms that contained tri-trophic food webs with phytoplankton, zooplankton, and planktivorous fish (bluegill, Lepomis macrochirus). We then induced treatments as described below (see Methods). We used a 2×2 factorial design that involved manipulating the presence/absence of fish predators and/or additional resources (i.e., fish carrion). This design created three perturbations, including predator removals (fish and carrion absent), resource pulses (fish and carrion present), and MMEs (fish absent and carrion present), as well as an experimental control (fish present and carrion absent), with 5 replicates each. We removed one replicate from the predator removal and resource pulse treatments because frogs deposited eggs and a harmful algal bloom occurred, respectively. We measured total productivity (chlorophyll-a), zooplankton assemblage characteristics and microalgae assemblage characteristics for 23 sample periods over 120 days.
Research sample	Each experimental replicate was a single freshwater mesocosm with locally-sourced phytoplankton and zooplankton and, depending on the treatment, the presence/absence of fish predators and/or fish carrion (see Study description). We used a mesocosm approach because it allowed for control and replication, as well as the controlled-inducement of a MME that directly affected a specific trophic level (i.e., only predators).
Sampling strategy	We were interested in understanding and comparing temporal dynamics following perturbations, which could be critical toward their differentiation, and thus we used a high-intensity sampling regime. Specifically, we collected 23 samples of chlorophyll-a , zooplankton, and microalgae (i.e., phytoplankton within the size range that are consumed by many dominant zooplankton consumers; see Methods: Sample collection) from each mesocosm. These samples involved 1 sample per week for three weeks, 2 samples per week for five weeks, and 1 sample per week for 10 weeks. We induced treatments (i.e., manipulated fish predators and/ or fish carrion) after the first 3 weeks (i.e., before the high intensity sampling period of 2 samples per week). The higher intensity sample period was intended to help elucidate potentially important transient dynamics following perturbations. We used a fluorometer to measure chlorophyll-a, an integrated tube sampler and light microscopy to enumerate zooplankton assemblage characteristics, and flow cytometry to enumerate microalgae assemblage characteristics. For all statistical analyses, we used smooth moving average data, as in similar studies, to reduce propagation of sampling error into temporal variation of response variables. This smooth moving average was based on three sample periods (i.e., the focal sample period, the previous period, and the subsequent period). Therefore, for the smoothed average data, there are only 20 sample periods because the first and last sample periods do not have previous or subsequent samples, respectively.
Data collection	The total number of samples and duration of the study were intended to thoroughly encapsulate the amount of time when limiting nutrients (e.g., N, P) are elevated in freshwater mesocosms after fish mortalities (see Methods: Freshwater mesocosms). For each chlorophyll-a sample, we obtained two samples and used the mean of these samples as the final value. For each zooplankton sample, we obtained characteristics for 10 individuals, or the most possible if fewer than 10, of each taxonomic family, which are often considered different functional groups. For each microalgae sample, we obtained characteristics for all individuals that could be identified to phylum within each 2-mL water sample (see Methods: Sample collection). Sample sizes for the mesocosm experiment were designed to be compatible with similar freshwater mesocosm experiments that used the same alpha value (0.05), while also being cognizant of researcher's logistical constraints and equipment availability.

Timing and spatial scale	The full experiment duration lasted from July 8th, 2019 to November 5th, 2019 (120 days). Zooplankton samples were obtained on the same day across mesocosms for each sample period. Chlorophyll-a and microalgae samples were collected over 2 different and consecutive days (i.e., 10 mesocosms per day) for each sample period. This staggered sampling protocol was necessary because of logistical and temporal constraints, namely the duration required to appropriately conduct flow cytometry.
Data exclusions	Two mesocosms were excluded from analyses: one from the predator removal treatment and one from the resource pulse treatment. These replicates were removed because of frog egg deposition and an algal bloom, respectively. The deposition of frog eggs resulted in many tadpoles that likely consumed zooplankton throughout the mesocosm. The algal bloom, while noteworthy, did not allow for proper comparisons of microalgae characteristics.
Reproducibility	We only performed the mesocosm experiment once. To facilitate the reproducibility of experimental findings, all code and data necessary for analyses are permanently available on public repositories. To ensure phytoplankton assemblages, zooplankton assemblages,, and (when applicable) fish predators were similar across mesocosms, we obtained phytoplankton and zooplankton from the same source lake and obtained similarly-sized fish from a local fish hatchery maintained by the Arkansas Game and Fish Commission (see Methods: Freshwater mesocosms).
Randomization	We haphazardly added the same volume of filtered lake water (i.e., phytoplankton) to each mesocosm to inoculate them with producers. Next, we used an aliquot to create zooplankton subsamples of similar volumes and compositions that were used to inoculate mesocosms with consumers. Lastly, we haphazardly assigned fish of similar size to each mesocosm prior to inducing treatments (see Methods: Freshwater mesocosms). Prior to the experiment, all mesocosms were haphazardly assigned treatments via a random number generator.
Blinding	Blinding of data acquisition and analyses were not necessary because data were collected by one researcher.

Did the study involve field work? ☒ Yes ☐ No

Field work, collection and transport

Field conditions	Field conditions throughout the experimental duration involved typical spring, summer, and fall weather conditions for northwest Arkansas, USA. Average daily temperature ranged from ~21°C in July 2019 (i.e., start of experiment) to ~5°C in November 2019 (i.e., end of experiment). Average total monthly precipitation over the time period was ~10 cm (Weather Underground). To protect mesocosms from excessive rainfall that could cause mesocosms to overflow, we covered each mesocosm with a water-resistant tarp during day(s) and night(s) when there was excessive rainfall.
Location	The experiment was conducted at an off-campus mesocosm site at the University of Arkansas at Fayetteville (36.115755, -94,142686).
Access & import/export	No permits were necessary to access the off-campus facility at the University of Arkansas at Fayetteville.
Disturbance	There were no intentional disturbances to freshwater mesocosms beyond the disturbances required to induce treatments as described in the "Study description". Specifically, we used an electroshocker to remove all fish predators across mesocosms and then, the following day, manipulated the presence/absence of fish predators and/or fish carrion to induce treatments (see Methods).

Reporting for specific materials, systems and methods

We require information from authors about some types of materials, experimental systems and methods used in many studies. Here, indicate whether each material, system or method listed is relevant to your study. If you are not sure if a list item applies to your research, read the appropriate section before selecting a response.

Materials & experimental systems

n/a	Involved in the study
☒	Antibodies
☒	Eukaryotic cell lines
☒	Palaeontology and archaeology
☐	☒ Animals and other organisms
☒	Clinical data
☒	Dual use research of concern

Methods

n/a	Involved in the study
☒	ChIP-seq
☐	☒ Flow cytometry
☒	MRI-based neuroimaging

Animals and other research organisms

Policy information about [studies involving animals](#); [ARRIVE guidelines](#) recommended for reporting animal research, and [Sex and Gender in Research](#)

Laboratory animals	The study did not involve laboratory animals.
Wild animals	The study involved wild-caught zooplankton and hatchery-reared fish predators (bluegill, Lepomis macrochirus). Zooplankton were collected from Lake Wilson near Fayetteville, Arkansas, USA, after which they were transported to the off-campus mesocosm facility described above. All zooplankton samples were reared in a separate freshwater mesocosm (with only phytoplankton added) until enough were collected to induce treatments (see Methods). All bluegill were obtained from the Arkansas Department of Game and Fish. Zooplankton and fish were reared in similar mesocosms until the experiment began.
Reporting on sex	Information about the age and sex of zooplankton were not assessed. Fish predators were about 1 year old and most individuals were male.
Field-collected samples	Laboratory work with field samples included measuring chlorophyll-a, enumerating preserved zooplankton samples, and using flow cytometry to enumerate microalgae. Both chlorophyll-a samples and microalgae samples were obtained from one much larger water sample obtained from each mesocosm for each sample period (see Methods: Sample collection). We prepared chlorophyll-a samples first and microaglae samples second, and both samples were prepared in indoor, room-temperature labs (~20°C). This process required two consecutive days to perform across mesocosms (i.e., prepare 10 mesocosms per day). Zooplankton samples were preserved in Lugol's solution and examined via light microscopy in either an indoor, room temperature lab or because of the pandemic, in a room-temperature home residence.
Ethics oversight	The Institutional Animal Care and Use Program (IACUC) at the University of Arkansas at Fayetteville approved the euthanasia procedure (IACUC #191060).

Note that full information on the approval of the study protocol must also be provided in the manuscript.

Flow Cytometry

Plots

Confirm that:

☐ The axis labels state the marker and fluorochrome used (e.g. CD4-FITC).

☐ The axis scales are clearly visible. Include numbers along axes only for bottom left plot of group (a 'group' is an analysis of identical markers).

☐ All plots are contour plots with outliers or pseudocolor plots.

☐ A numerical value for number of cells or percentage (with statistics) is provided.

Methodology

Sample preparation	*Describe the sample preparation, detailing the biological source of the cells and any tissue processing steps used.*
Instrument	*Identify the instrument used for data collection, specifying make and model number.*
Software	*Describe the software used to collect and analyze the flow cytometry data. For custom code that has been deposited into a community repository, provide accession details.*
Cell population abundance	*Describe the abundance of the relevant cell populations within post-sort fractions, providing details on the purity of the samples and how it was determined.*
Gating strategy	*Describe the gating strategy used for all relevant experiments, specifying the preliminary FSC/SSC gates of the starting cell population, indicating where boundaries between "positive" and "negative" staining cell populations are defined.*

☐ Tick this box to confirm that a figure exemplifying the gating strategy is provided in the Supplementary Information.